12. ERATOSTHENIAN SYSTEM

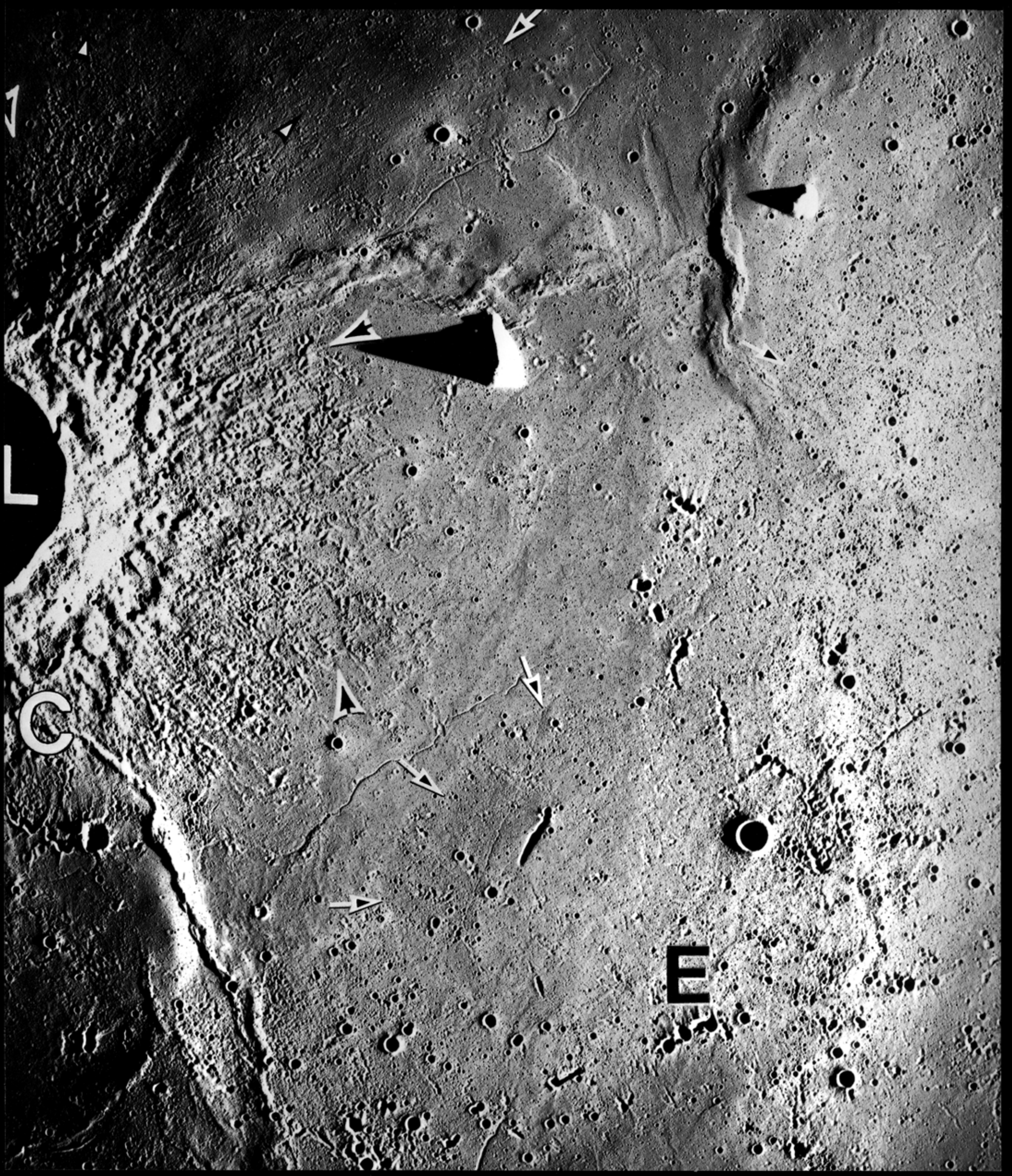

FIGURE 12.1 (OVERLEAF). — Eratosthenian crater and mare materials. L, Lambert (30 km), superposed on Imbrian mare units (small white-on-black arrowheads) and embayed by Eratosthenian mare units (large black-on-white arrowheads). Mare unit containing sinuous rille has a D_L value of 220 ± 45 m (Boyce, 1976), floods southeastern secondary craters of Lambert, and covers older mare unit (three black-on-white arrows pointing southeastward). Older unit underlies secondaries of Eratosthenes (E). Therefore, stratigraphic relations of Lambert and Eratosthenes are similar; crater densities (fig. 12.4) distinguish Lambert (older) from Eratosthenes (younger). Secondary craters of Copernicus (C) are superposed on Lambert. Apollo 15 frame M–1009.

12. ERATOSTHENIAN SYSTEM

CONTENTS

INTRODUCTION

The two time-stratigraphic units described here and in the next chapter are less extensive than the four already described. The contrast in rates of formation is even greater: The Eratosthenian and Copernican Systems combined required three times longer to form than did the four previous units combined. The Eratosthenian and, to a lesser extent, the Copernican Systems continue the geologic style of the Upper Imbrian Series. Eratosthenian mare and crater materials are both present; the maria are about twice as extensive as the crater deposits (pl. 10).

Because the Eratosthenian and Copernican rock units are relatively young, they are little modified. Each crater deposit is visible farther from the rim crest than are older crater deposits, because the topography has been less eroded and the materials less completely mixed with the substrate. Eratosthenian and Copernican units serve as models for interpretations of the older units because of their freshness and clear stratigraphic relations (fig. 12.1).

In a sense, all the sampling missions obtained samples of Eratosthenian and Copernican material because they returned regolith material (Heiken, 1975; Papike and others, 1982). Many minor impacts have been dated either individually or collectively by determining the duration of exposure of regolith particles (Arvidson and others, 1975; Burnett and Woolum, 1977; Crozaz, 1977). However, Eratosthenian and Copernican bedrock units (those visible on regional photographs) were only sparsely sampled. Mare-basalt flows believed to be Eratosthenian were sampled only at the Apollo 12 landing site. No large Eratosthenian craters were sampled, and large Copernican craters were sampled only indirectly (see chap. 13). Therefore, the reconstruction of post-Imbrian geologic history requires considerable photogeologic extrapolation—a process not yet complete.

DEFINITION

Shoemaker and Hackman (1962) established the craters Eratosthenes and Copernicus as the type areas of the Moon's two youngest time-stratigraphic systems because of stratigraphic relations evident on telescopic photographs. Ejecta of Eratosthenes is superposed on the nearby mare material, whereas rays of Copernicus are superposed on Eratosthenes (figs. 1.1, 1.6, 12.2). Eratosthenes is much the darker of the two craters on full-Moon photographs (fig. 12.2*B*) and was thought to be rayless. Although one faint ray, in fact, extends northwestward from the crater (formed by a long linear chain of secondary craters visible in fig. 11.3), Eratosthenes nevertheless does represent a class of postmare craters that essentially lack bright rays.

Accordingly, postmare craters have been operationally divided in most lunar geologic mapping into Eratosthenian and Copernican categories according to whether they are nonrayed or bright-rayed, respectively. Although ray visibility is neither exact nor correct as a criterion of age according to the stratigraphic code,[12.1] it has yielded many subsequently confirmed age estimates and is still useful where better data are unavailable.

Neither Shoemaker and Hackman (1962) nor later work have established the stratigraphic position of Eratosthenes and Copernicus within their respective systems. Wilhelms (1980) attempted to define or, at least, to better characterize the two systems on the basis of units in southern Mare Imbrium and northern Oceanus Procellarum. A stratigraphic sequence was established (fig. 7.1; table 7.2), and the existing age assignments of as many units as possible were retained. The definitions were based on mare units because, in this region, they are more extensive and lithologically uniform than impact deposits. Because time-stratigraphic units are contiguous, the working criterion for mare units at the top of the Imbrian System, $D_L = 240 \pm 10$ m, also characterizes the base of the Eratosthenian System (table 12.1). Mare units having these or smaller D_L values are post-Imbrian. Though not a formally acceptable criterion, the D_L values are at least a secondary (superposed) criterion that is a function of time.

Although fewer crater frequencies than D_L values are available for individual Eratosthenian units, the frequencies determined by Neukum and others (1975a, b) and Neukum and König (1976) probably represent the approximate range of Eratosthenian frequencies[12.2]. A plot of many of their determinations suggests that a crater frequency of 2.5×10^{-3} corresponds approximately to the borderline D_L value of 240 m (fig. 7.15) and thus should characterize the mare

[12.1]The stratigraphic code (American Commission on Stratigraphic Nomenclature, 1970) was partly adhered to as follows. Rays were considered to be a physical characteristic by which *rock*-stratigraphic units may be legitimately defined. Each ray deposit or ejecta deposit from which rays emanate was considered to be a formation and could be mapped by objective criteria, as should all formations. Then, the formations were assigned *time*-stratigraphic significance according to the physical property of the presence or absence of rays; all materials of postmare nonrayed craters were lumped on a map as Eratosthenian, and all materials of rayed craters as Copernican. Before Lunar Orbiter photographs were available in 1966-67, rayless but topographically fresh craters not in contact with mare units were commonly assigned an indefinite Imbrian or Eratosthenian age (map unit EIc). The fact that some crater ages were incorrectly estimated by the ray criterion illustrates the validity of the code's insistence on the separation of rock and time-rock categories of units.

[12.2]Except as noted, all crater frequencies given in this chapter refer to cumulative numbers of craters 1 km in diameter and larger per square kilometer. Neukum and his coworkers obtained these frequencies by normalizing their crater size-frequency curves at this 1-km intercept.

TABLE 12.1.—*Properties of craters superposed on units of the Eratosthenian System*

[Frequencies are those of craters at least 1 km in diameter per square kilometer, as determined by normalization to 1 km by means of a calibration curve (see fig. 7.10G; Neukum and others, 1975a); n.a., not available]

Boundary	Substrate	Frequency	Basis	D_L (m)	Basis	Age (aeons)	Basis
Upper	Crater material	10^{-3}	Figure 12.4	180±20	Table 12.3	1.1	Chapter 13.
	Mare basalt	n.a.	---	≤165±25	Youngest flows traditionally considered Eratosthenian		
Lower	Crater material	$1\text{-}2\times10^{-2}$	Figure 12.4	≥310	Table 12.3	3.2	Between Apollo 12 and 15 ages.
	Mare basalt	2.5×10^{-3}	Table 11.1	240±10	Consistent with traditional mapping of crater and mare units (Wilhelms, 1980)		

materials at the base of the Eratosthenian System (table 12.1). Some flows in Oceanus Procellarum and Mare Imbrium with D_L values smaller than 240 m were found to have frequencies of 1 to 2×10^{-3} (figs. 12.3, 12.4*A*, *E*; Neukum and König, 1976; Gerhard Neukum, written commun., 1979). A further indication that a crater frequency of 2.5×10^{-3} and a D_L value of 240 m are equivalent for the system's base is the finding (with a large uncertainty) of a crater frequency of 2.6×10^{-3} on the upper Upper Imbrian mare unit(s) at the Apollo 15 landing site, where $D_L = 270\pm15$ m (table 11.1; figs. 11.2, 12.4*B*, *C*).

The top of the system is harder to characterize. Wilhelms (1980) employed a D_L value of 140 m as a working criterion for the Eratosthenian-Copernican boundary, based on values of 165 ± 25 m that were measured on the youngest mare units in Mare Imbrium traditionally called Eratosthenian (Boyce and others, 1975). However, smaller values may eventually be found. Similarly, the small frequencies found for some young flows (fig. 12.3) may not be the smallest that exist.

In summary, D_L values for Eratosthenian mare materials range from less than 140 m to 240 ± 10 m, and the frequencies of craters at least 1 km in diameter per square kilometer (normalized) range as high as to 2.5×10^{-3}. The values for crater materials of the same age differ (table 12.1), as shown in the next section.

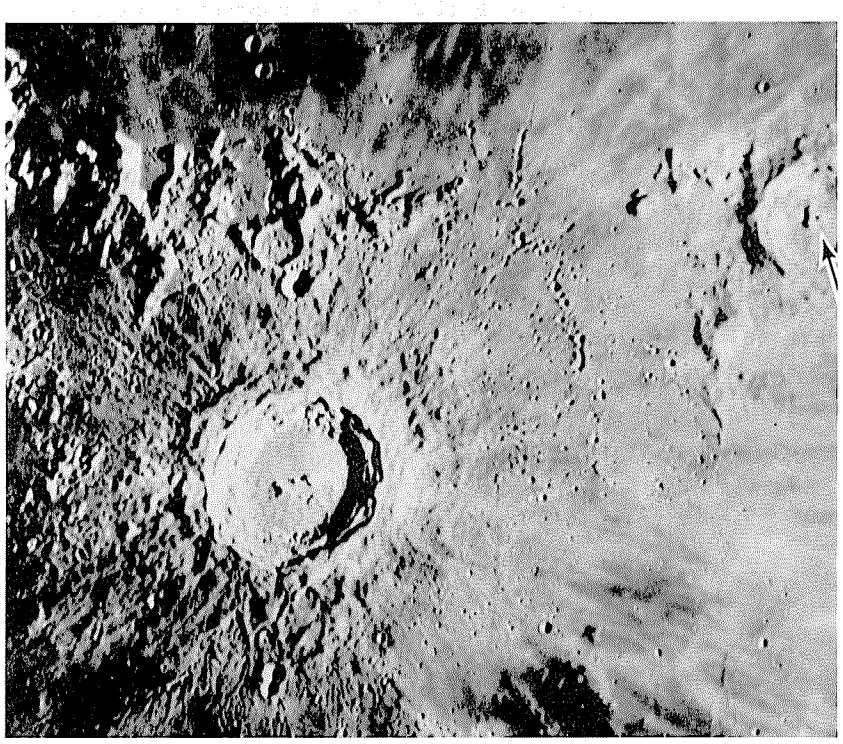

A

B

CRATER MATERIALS

Recognition criteria

The best criteria for an Eratosthenian age of a crater deposit are stratigraphic relations with the mare materials. Eratosthenian mare and crater deposits interfinger on much of the central and western nearside. Excellent examples of these relations are in Mare Imbrium (figs. 7.4, 12.1, 12.5; table 7.2) and Oceanus Procellarum (fig. 12.6). Extensive flows with D_L values smaller than 230 m overlap Lambert and other craters that traditionally have been mapped as Eratosthenian (fig. 12.1; Wilhelms, 1980). However, the fresh bright craters Euler and Timocharis, previously considered to be Copernican, are also overlapped by such flows (fig. 7.4). These and other stratigraphically inconsistent assignments have been revised according to the philosophy of preserving a maximum number of existing assignments. The extensive mare materials remain Eratosthenian, and the few embayed bright craters become Eratosthenian (table 12.2).

Crater counts made marginally feasible by the best Lunar Orbiter and Apollo photographs (fig. 12.4; Neukum and König, 1976) can date favorably situated craters. Neukum and König (1976) found that the ages assigned to large rayed craters by the criteria of rays and

C

FIGURE 12.2.—Superposition of Copernicus rays and secondary craters on Eratosthenes; arrows mark same point in each photograph.
A. Low-Sun telescopic photograph.
B. High-Sun telescopic photograph. Eratosthenes is almost invisible. White arrowhead marks radial ray. CH, Copernicus H (compare fig. 13.6).
C. Part of Orbiter 4 frame H–114.

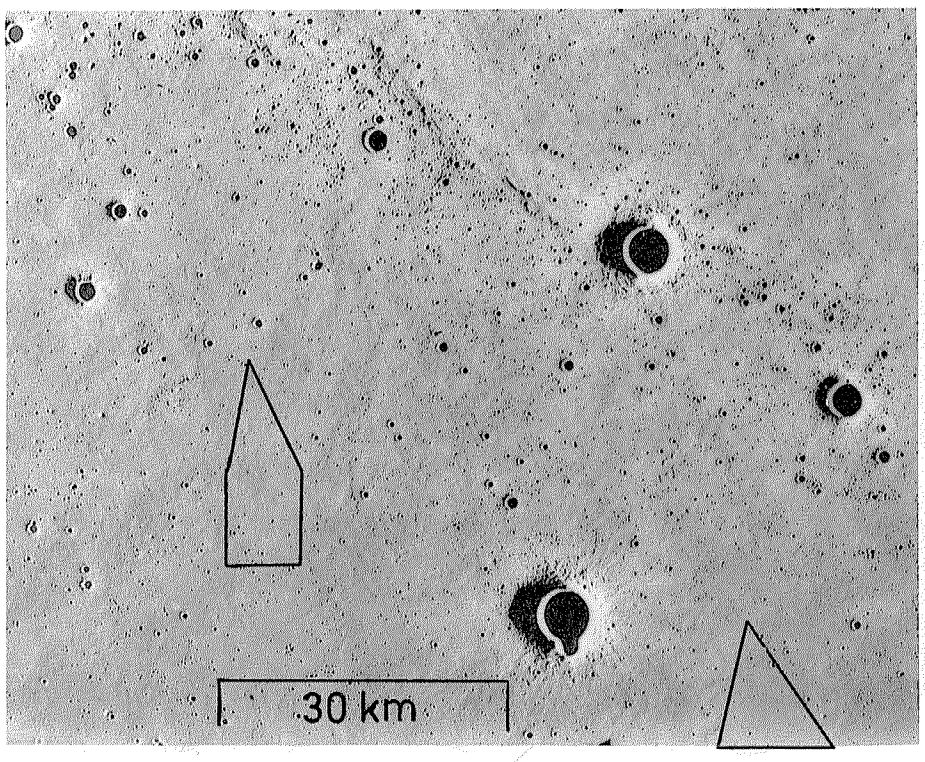

A

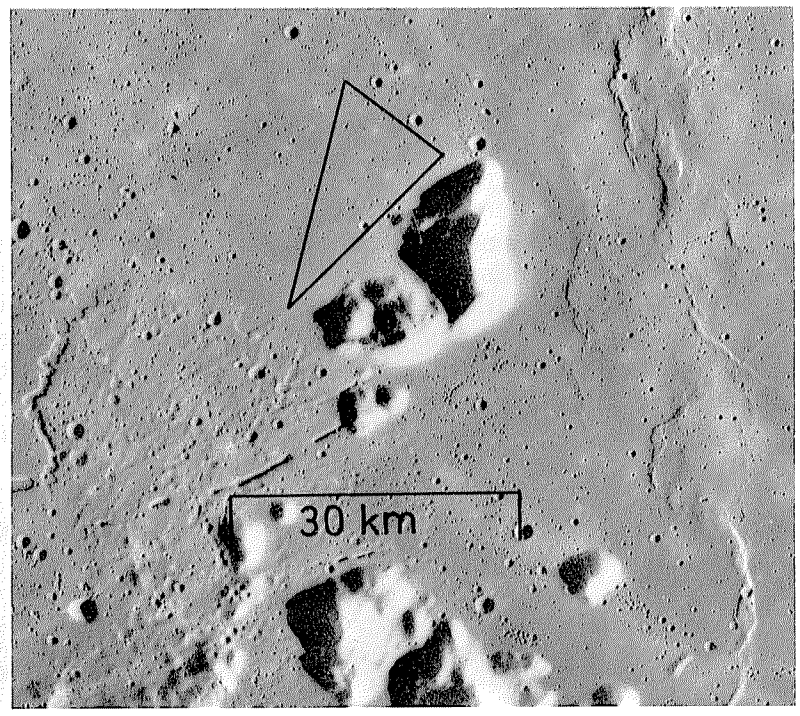

B

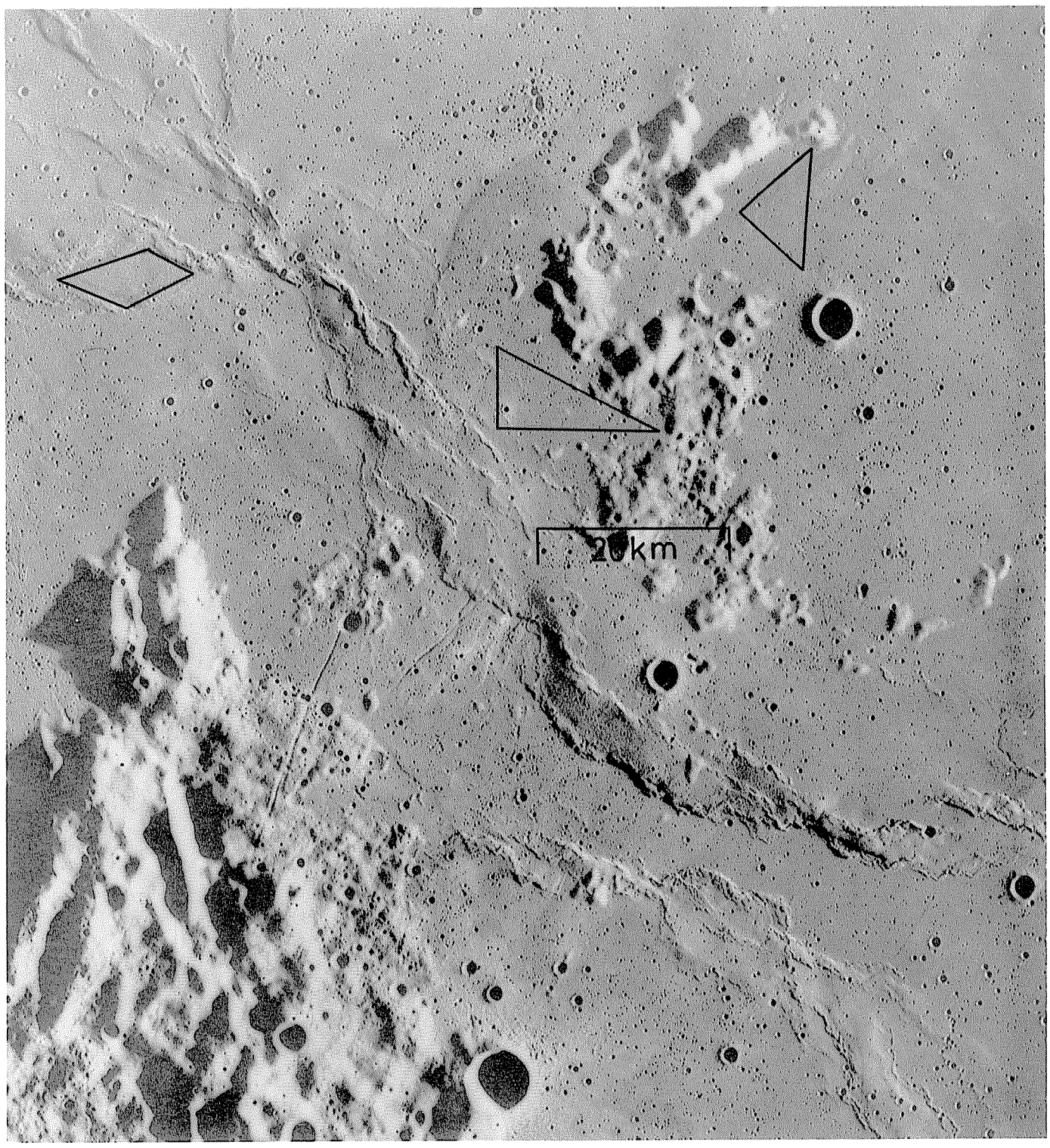

C

FIGURE 12.3.—Eratosthenian mare materials in Oceanus Procellarum, showing areas included in crater counts by Neukum and others (1975a, b) and Neukum and König (1976). Courtesy of Gerhard Neukum.

A. Northern Procellarum. Scene centered at 26.5° N., 62.5° W.

B. Montes Harbinger, at border between northern Procellarum and Mare Imbrium. Crater-count area centered at 27.5° N., 41.5° W.

C. Southern Procellarum, near crater Letronne (large rugged area at lower left). Scale bar at 10° S., 38.5° W., over island probably belonging to Flamsteed-Billy basin.

morphology were consistently too young, probably because the rays and the sharpness and roughness of the coarse-textured crater subunits give the impression of youth. Langrenus (fig. 9.5), Theophilus (fig. 11.1), and several other large rayed craters are here accepted as Eratosthenian because their crater densities are similar to those on Lambert (fig. 12.1) and Bullialdus (fig. 12.7), which are sandwiched between Eratosthenian and young Imbrian mare materials.

Crater frequencies as high as 2×10^{-2} were found to be superposed on craters traditionally mapped as Eratosthenian (fig. 12.4). This and other frequencies for Eratosthenian craters are substantially larger than the frequencies of 2.5×10^{-3} superposed on mare materials at the base of the Eratosthenian System. The curve for the Apollo 15 units, just below the system's base, lies amidst the frequency plots for many typical Eratosthenian craters and even for some Copernican craters (fig. 12.4*B*, *C*). Different crater frequencies, therefore, seem to apply to mare and crater materials (Ahrens and Watt, 1980).

The 18-km-diameter crater Diophantus is a borderline case near the upper boundary of the Eratosthenian System. Diophantus has no visible rays (fig. 2.2), is younger than the youngest Eratosthenian flows shown in figure 2.2 by an unknown amount, and has not been flooded by younger mare units. It has been retained in the Eratosthenian System because that was its longstanding assignment (Wilhelms and McCauley, 1971) and because no reason for a change is apparent (Wilhelms, 1980). Diophantus is the youngest crater here considered to be Eratosthenian for which, to my knowledge, superposed crater frequencies have been accurately determined ($1.25\pm0.5\times10^{-3}$; fig. 12.4*D*, *E*; Neukum and König, 1976). Thus, this

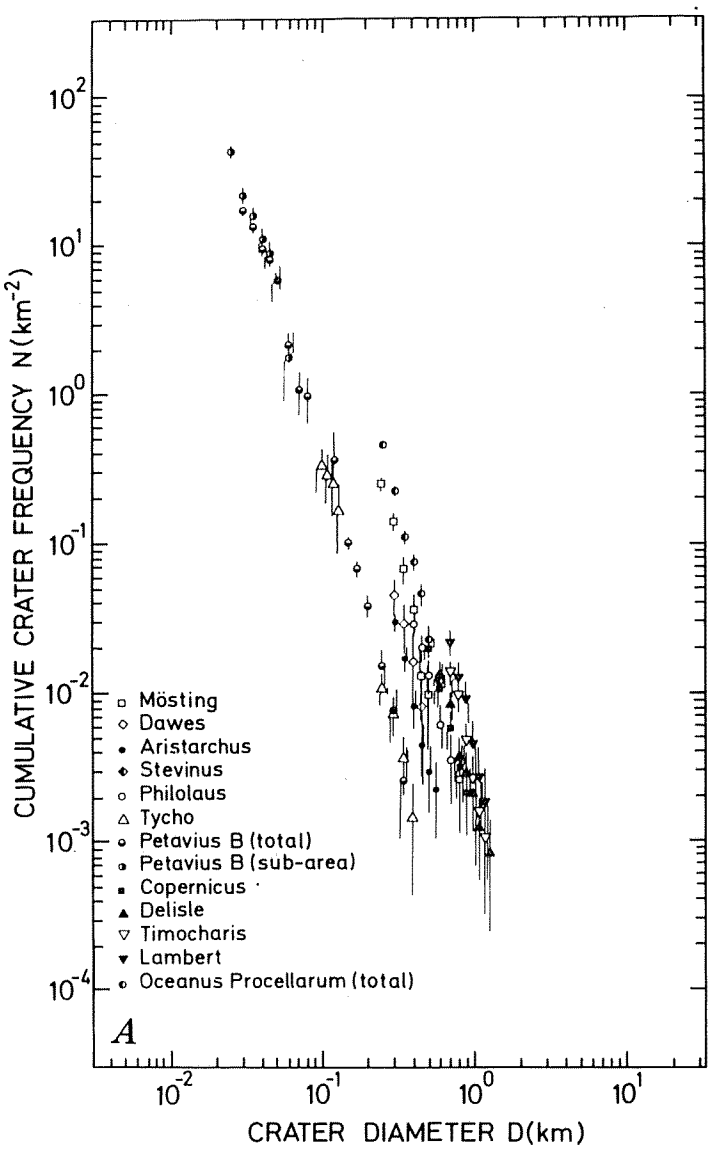

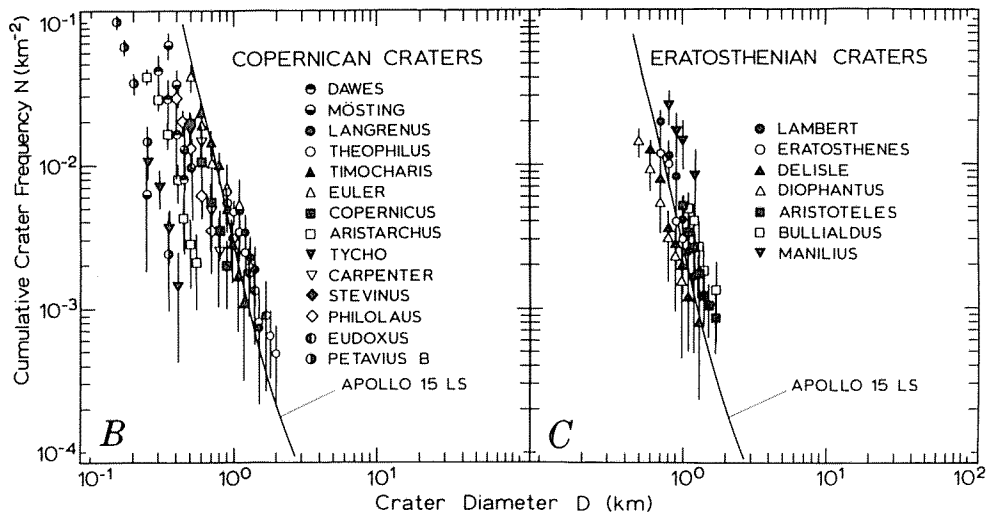

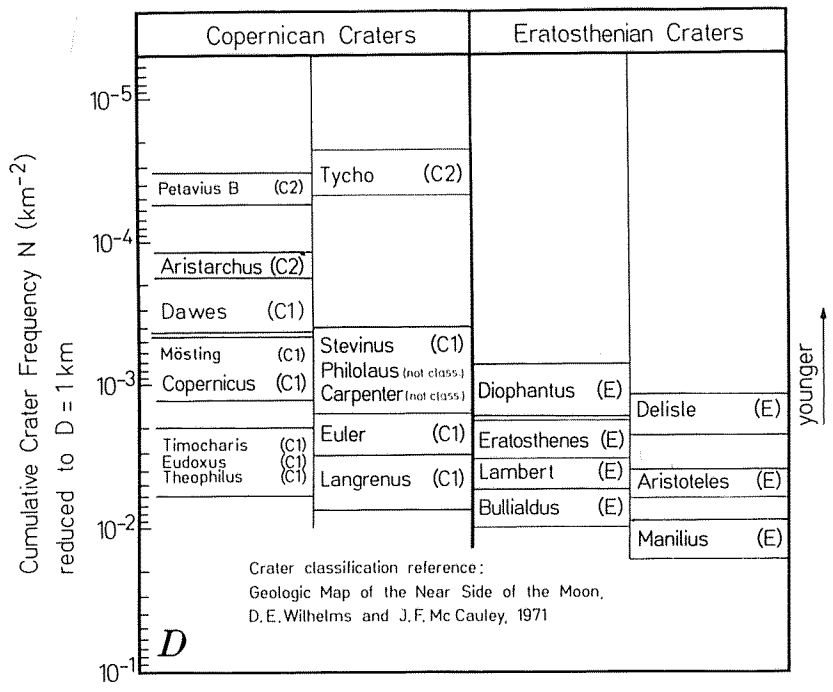

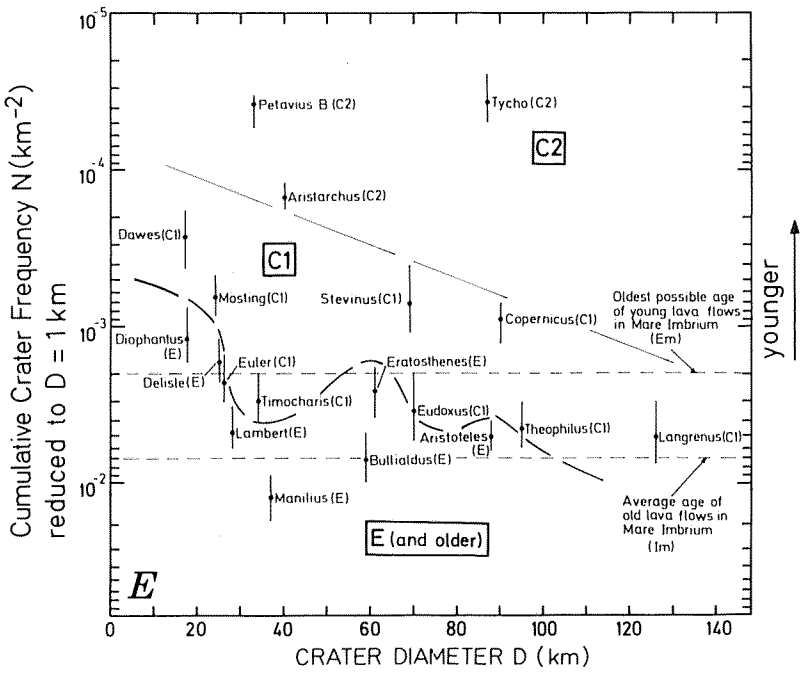

FIGURE 12.4.—Crater-frequency studies by Neukum and König (1976) of large craters mapped as Eratosthenian and Copernican by Wilhelms and McCauley (1971).

A. Plots for some craters relative to curve for mare materials of Oceanus Procellarum (total of areas in fig. 12.3 and of other areas not shown).

B. Plots for Copernican craters relative to curve for mare material at Apollo 15 landing site (LS; compare fig. 11.2). Mare curve is intermediate in group of apparent ages; mare and crater materials with same superposed-crater frequencies differ in age.

C. Similar plots for craters considered to be Eratosthenian by Wilhelms and McCauley (1971).

D. Age assignments (E, C1, C2) by Wilhelms and McCauley (1971); ranking by Neukum and König (1976), youngest at top.

E. Same craters plotted by age (youngest at top) and size (horizontal axis), showing probable bias to too-young age assignments of such large craters as Langrenus and Theophilus.

TABLE 12.2.—*Representative Eratosthenian craters*

[Cross rules divide diameter ranges mapped differently in plate 10: smaller than 30 km, unmapped; 30 to 59 km, interiors mapped; 60 km and larger, exterior deposits mapped. UI, possibly Upper Imbrian]

Crater	Diameter (km)	Center (lat)	Center (long)	Figure	Remarks
Maestlin G-----	3.5	2° N.	42° W.	12.6	---
Taruntius H----	9	0.5° N.	50° E.	3.2B	---
Bessarion B----	12	17° N.	42° W.	3.14A	Double impact.
Cayley---------	14	4° N.	15° E.	10.3B	---
Brayley--------	15	21° N.	37° W.	12.5	Rim flooded.
Diophantus-----	18	28° N.	34° W.	2.2	See figure 12.4; table 7.2.
Peirce---------	19	18° N.	54° E.	5.23, 9.11	---
Flamsteed------	21	5° S.	44° W.	12.6A	Clear stratigraphy.
Picard---------	23	15° N.	55° E.	9.11	---
Delisle--------	25	30° N.	35° W.	2.2	See figure 12.4; table 7.2.
Arago----------	26	6° N.	21° E.	3.2C	---
Euler----------	28	23° N.	29° W.	1.6, 3.29, 7.4	See figure 12.4; table 7.2.
Lambert--------	30	26° N.	21° W.	1.6, 6.4, 12.1	See figure 12.4; tables 7.2, 12.3.
Reiner---------	30	7° N.	55° W.	12.10	Asymmetric.
Archytas-------	32	59° N.	5° E.	10.15	---
Timocharis-----	34	27° N.	13° W.	1.6, 11.3	See figure 12.4; tables 7.2, 12.3.
Stearns--------	37	35° N.	163° E.	12.9	Farside example.
Manilius-------	39	15° N.	9° E.	1.7, 10.16	See figure 12.4; table 12.3.
Herschel-------	41	6° S.	2° W.	7.7	See table 12.3.
Rothmann-------	42	31° S.	28° E.	11.5, 11.7	---
Plinius--------	43	15° N.	24° E.	5.17	See table 12.3.
Reinhold-------	43	3° N.	23° W.	13.10	Do.
Agrippa--------	44	4° N.	11° E.	10.16	Do.
Hainzel A------	53	41° S.	34° W.	9.24	Do.
Maunder--------	55	15° S.	94° W.	3.15A, 4.4B	Typical.
Eratosthenes---	58	15° N.	11° W.	1.6, 11.3, 12.2	Typical (see fig. 12.4; tables 7.2, 12.3).
Bullialdus-----	61	21° S.	22° W.	12.7	See figure 12.4; table 12.3.
Hercules-------	69	47° N.	39° E.	1.7, 9.3	Mare fill.
Werner---------	70	28° S.	3° E.	1.8, 3.26, 7.7, 9.27	Typical.
Fabricius------	78	43° S.	42° E.	8.5	UI?
Aristoteles----	87	50° N.	17° E.	1.7, 10.12	See figure 12.4.
Theophilus-----	100	11° S.	26° E.	11.1	Rayed (see fig. 12.4; table 12.3).
Pythagoras-----	130	64° N.	63° W.	1.6, 10.2	---
Langrenus------	132	9° S.	61° E.	9.5	Rayed (see fig. 12.4).
Hausen---------	167	66° S.	88° W.	3.2E	Largest young crater.

frequency approximates, but does not specify, the frequency of craters superposed on crater materials at the Eratosthenian-Copernican boundary. The total range for Eratosthenian crater deposits is, therefore, about 7.5×10^{-4} to 2×10^{-2}; most midpoint values lie between 10^{-4} and 10^{-3} craters.

D_L values for crater deposits scatter widely (fig. 12.8; table 12.3). Including error bars, the range for Eratosthenian units is 130 to 330 m; midpoints range from 160 to 310 m. Like the frequencies, therefore, the D_L values apparently are displaced toward larger values for

TABLE 12.3.—*Properties of craters superposed on larger crater deposits*

[Orbiter frames listed are those used for D_L determinations and differ from those used for crater-frequency counts.
Ages: C, Copernican; E, Eratosthenian (pls. 10, 11).
Crater frequencies are from Neukum and König (1976) (see fig. 12.4); they refer to craters at least 1 km in diameter per square kilometer, as determined by normalization to 1 km by means of a calibration curve (see fig. 7.10G; Neukum and others, 1975a).
D_L values determined by J.M. Boyce]

Crater	Diameter (km)	Orbiter frame	Age	Crater frequency	D_L (m)
Tycho----------	85	5 H-128	C	3.7×10^{-5}	20±10
Aristarchus-----	40	5 H-201	C	1.5×10^{-4}	50±10
Kepler----------	32	5 H-138	C	---	75±10
Copernicus------	93	5 H-146	C	9.0×10^{-4}	100±30
Gassendi A------	33	5 H-180	C	---	100±15
Eudoxus---------	67	4 H-98	C	3.6×10^{-3}	120±30
Godin-----------	35	4 H-97	C	---	130±20
Aristillus------	55	4 H-103	C	---	140±30
Timocharis------	34	4 H-114	E	3.0×10^{-3}	160±30
Bürg------------	40	4 H-86	C	---	175±35
Autolycus-------	39	4 H-103	C	---	180±20
Herschel--------	41	4 H-108	E	---	180±20
Manilius--------	39	4 H-97	E	1.3×10^{-2}	185±40
Horrocks--------	31	4 H-96	E	---	200±20
Bullialdus------	61	4 H-125	E	7.0×10^{-3}	215±25
Plinius---------	43	4 H-85	E	---	215±35
Cichus----------	41	4 H-124	E	---	215±65
Reinhold--------	43	4 H-125	E	---	245±35
Lambert---------	30	4 H-126	E	4.8×10^{-3}	250±10
Theophilus------	100	4 H-77	E	4.6×10^{-3}	260±40
Eratosthenes----	58	5 H-134	E	2.7×10^{-3}	270±60
Lexell----------	63	4 H-107	E	---	260±20
Agrippa---------	44	4 H-97	E	---	265±55
Hainzel A-------	53	4 H-136	E	---	310±20

crater substrates than for mare substrates (compare total range of 140 to 250 m, table 12.1).

Small craters are identified as Eratosthenian by the criteria of Trask (see chap. 7), which were also devised by observing the relations of craters to mare materials. Small Eratosthenian craters are buried in many places by mare flows on which other Eratosthenian craters are superposed (figs. 12.5, 12.6).

In most farside and some limb regions, where photographs are poor, crater assignments to the Eratosthenian are still based on qualitative estimates of a low crater density, coupled with fresh morphology and an absence of detectable rays. The fine texture of radial ejecta and secondary craters is probably the morphologic feature most sensitive to degradation by small impacts and thus is most

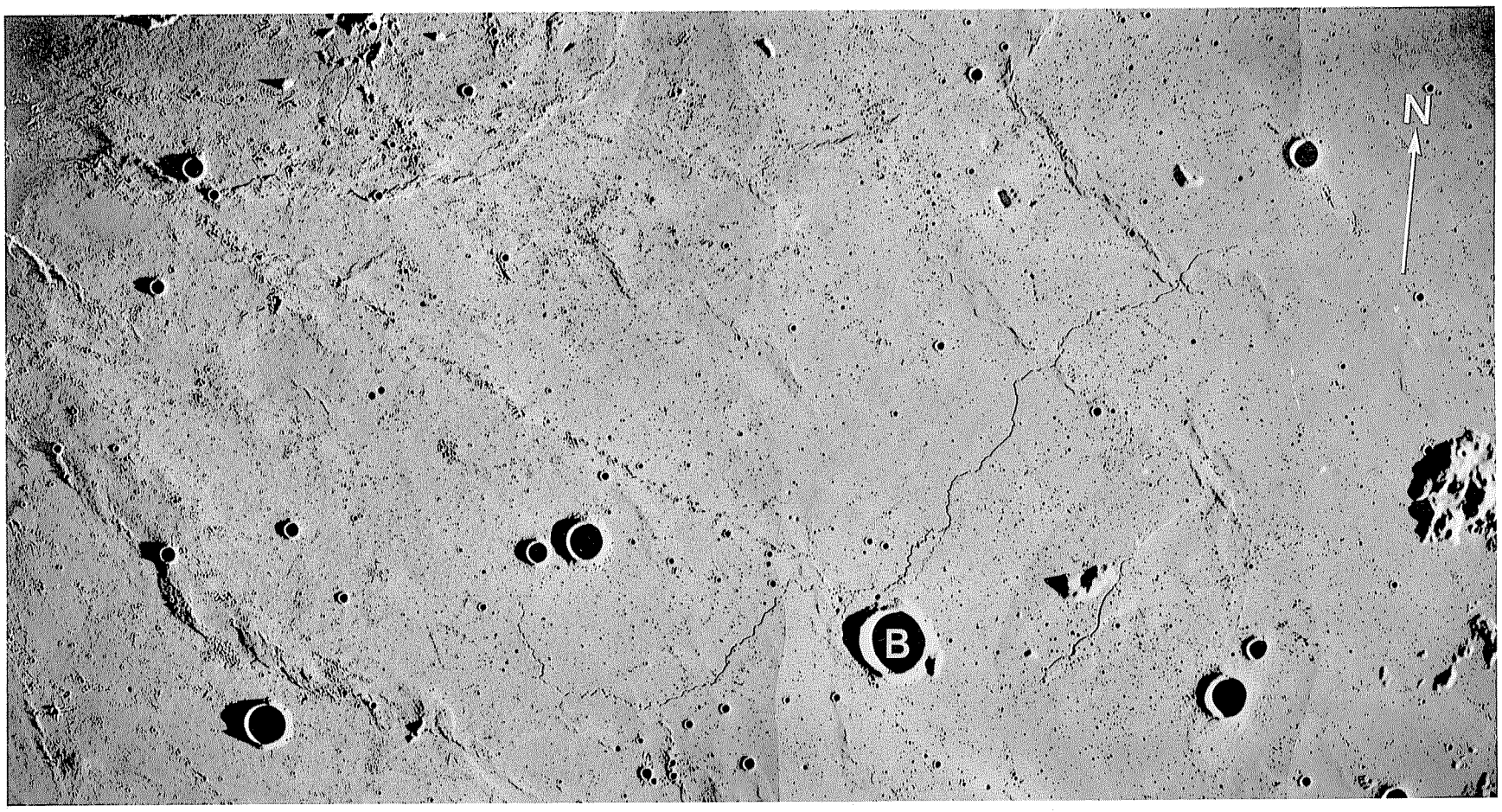

FIGURE 12.5.—Extensive Eratosthenian mare materials in southern Mare Imbrium, flooding rim materials of many small Eratosthenian craters, the largest of which is Brayley (B; 15 km, 21° N., 37° W.). Long chain of secondary craters extends northwestward of Brayley radial to Aristarchus, just outside left edge of photograph. Parts of Imbrium-basin rings are exposed as rugged terra islands. Mosaic of Apollo 17 frames M–2925, M–2928, and M–2931 (from right to left).

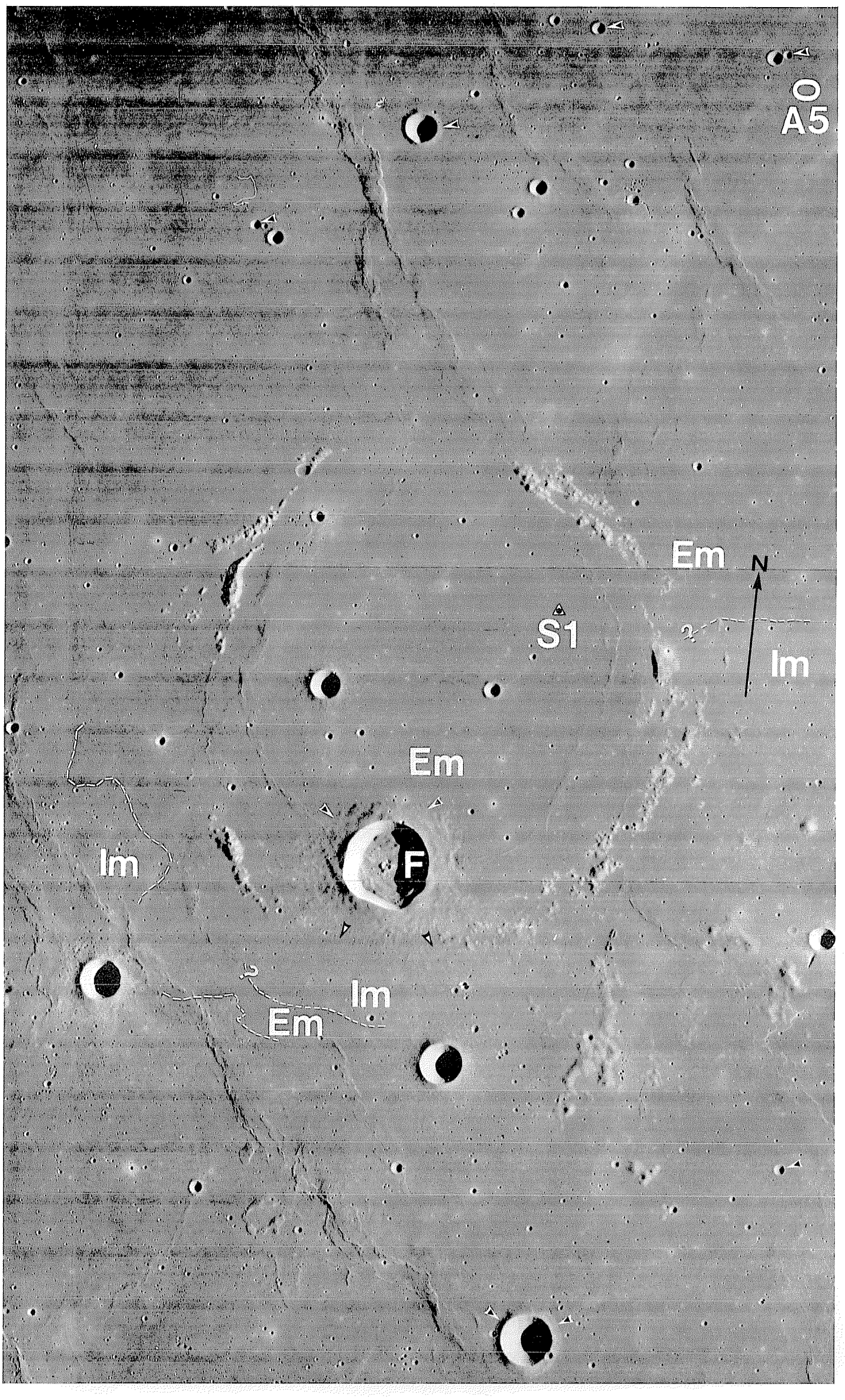

FIGURE 12.6.—Part of Oceanus Procellarum near crater Flamsteed.

A. Large ring of rounded hills is Flamsteed P (112 km), a nearly buried pre-Imbrian (Nectarian or pre-Nectarian) crater. Eratosthenian crater Flamsteed (F; 21 km) is superposed on Imbrian (Im) mare unit in south (white-on-black arrowheads) and embayed by younger Eratosthenian (Em) mare unit in north (black-on-white arrowheads). Other embayments of Eratosthenian or Imbrian craters are also shown by black-on-white arrowheads. Dashed lines indicate subtle contacts between Em and Im units; mare is closer to rims of small craters in Em than in Im, and crater density is lower in Em. S1, Surveyor 1 landing site; A5 (ellipse), potential Apollo landing site 5. Orbiter 4 frame H–143.

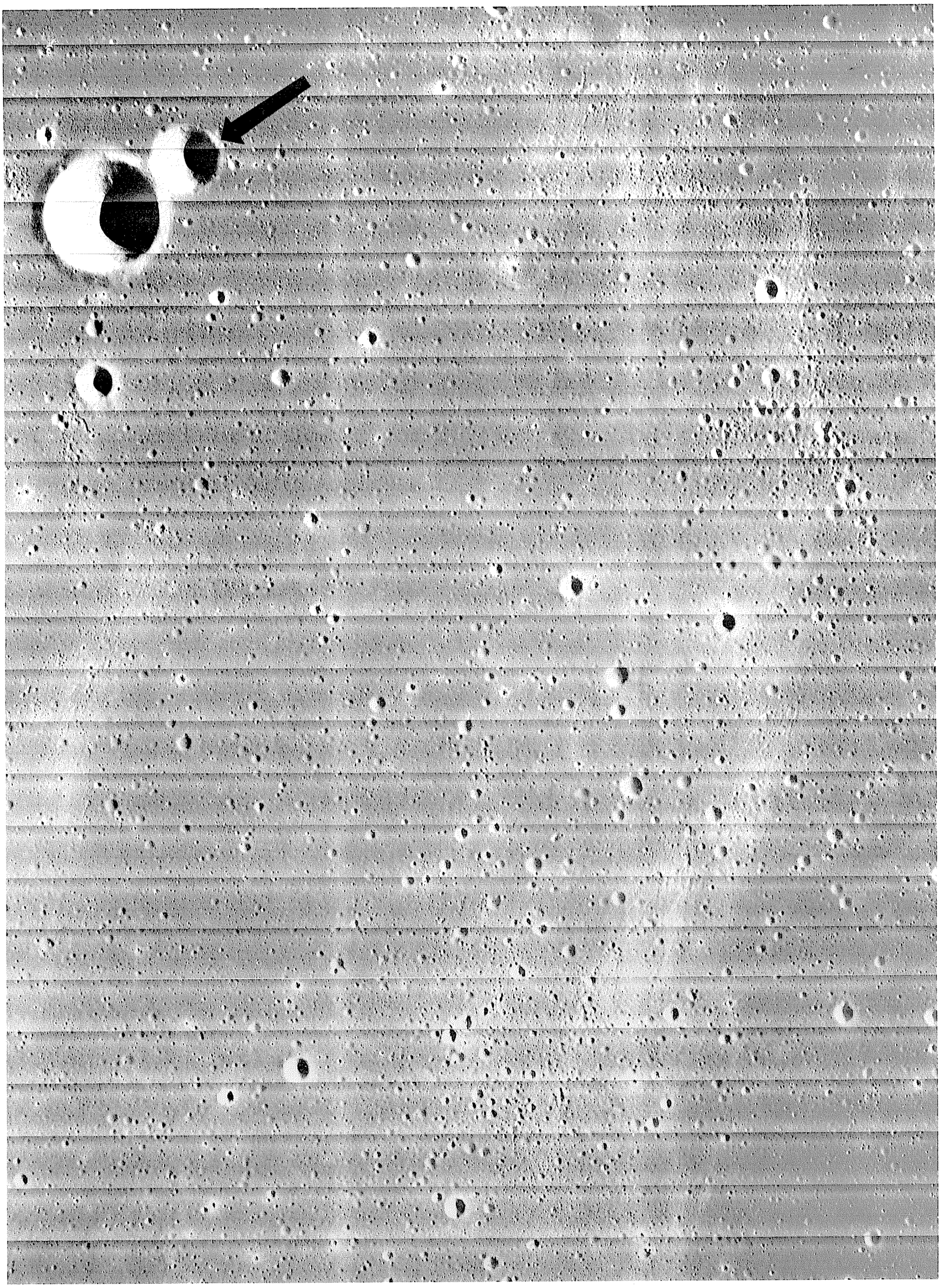

B. Arrow indicates embayment of pair of otherwise fresh-appearing small craters also shown by black-on-white arrowhead above ellipse A5 in *A*. Largest crater is Maestlin G (3.5 km). Extensive level terrain, despite numerous small craters, indicates that no craters larger than 200 m in diameter are degraded to saucer shapes, as would be true on an Imbrian mare surface. Heavily cratered streak extending over most of right half of photograph is ray of crater Kepler (Carr and Titley, 1969), 200 km away in direction indicated by herringbone pattern. Orbiter 2 frame M–207.

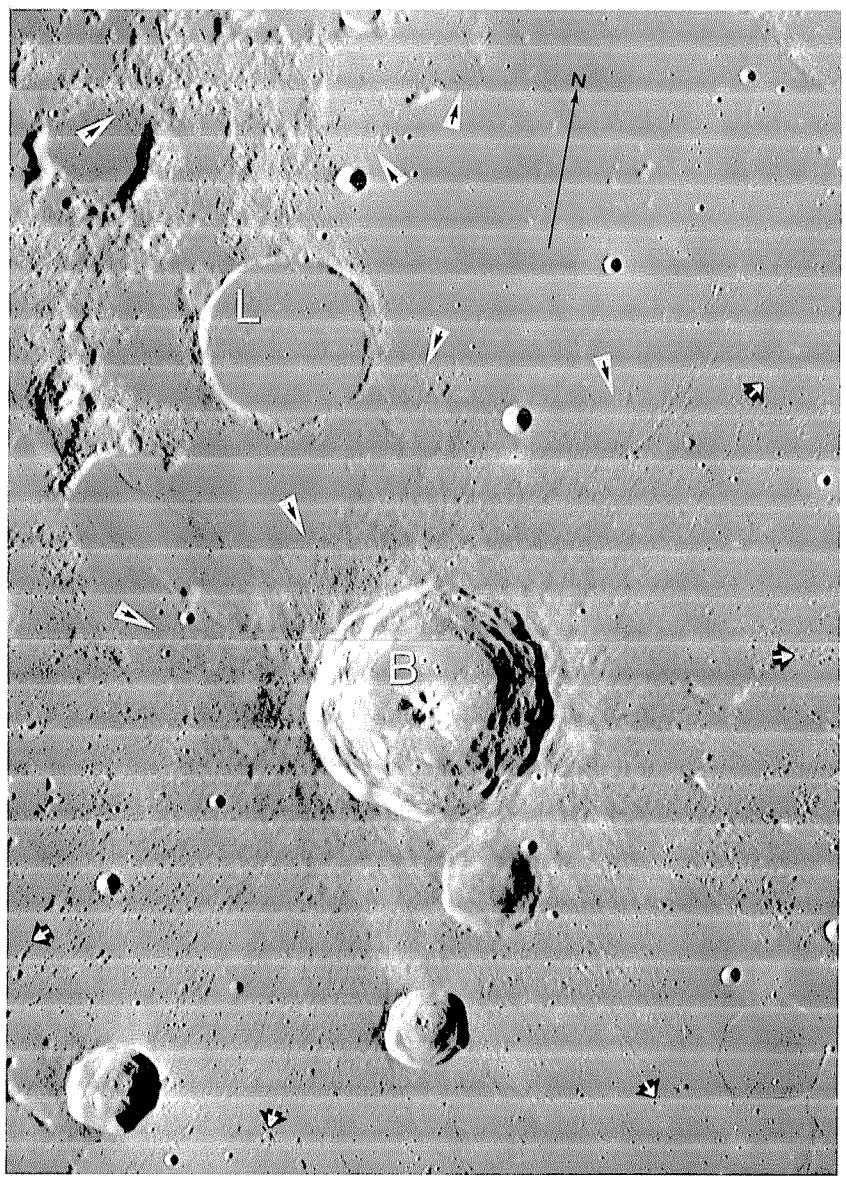

FIGURE 12.7.—Eratosthenian crater Bullialdus (B; 61 km), superposed on Imbrian mare materials (white-on-black arrows) and embayed by Eratosthenian mare materials (black-on-white arrows). Crater Lubiniezky (L; 44 km) is filled by thin mare unit younger than Bullialdus-secondary craters; embayment relations are traceable northwest and northeast of Lubiniezky. Orbiter 4 frame H–125.

diagnostic (fig. 12.9). Where neither this fine texture nor crater densities are visible, ray brightness is still used for dating. The inconsistencies in dating uncovered by Neukum and König (1976) illustrate that the morphologies of Late Imbrian, Eratosthenian, and early Copernican craters of subequal sizes differ only slightly when seen on any but the best photographs. Theophilus and Langrenus, for example, would still be considered Copernican if they were on parts of the farside not covered by Apollo photographs and if their rays were visible against the terra background.

Among the Eratosthenian craters dated by size-frequency studies is Cavalerius (fig. 12.10; D.B. Snyder, written commun., 1980). The peculiar bright feature in Oceanus Procellarum called Reiner gamma may be an exceptionally bright part of the otherwise-faint ray pattern of Cavalerius (fig. 12.10; Hood and others, 1979). Reiner gamma has been thought to be Copernican because of its brightness and superposition on other features (McCauley, 1967a). Interest in the origin of this enigmatic feature has been revived by the discovery that it has the highest magnetism yet observed from lunar orbit (Hood and others, 1979). The Eratosthenian age of Reiner gamma, if confirmed, would constrain speculations about the origin of lunar magnetism, one of the major unsolved problems raised by Apollo exploration. It also would illustrate a failure of the bright-ray criterion for distinguishing Eratosthenian and Copernican ages.

Some of the physical explanations first proposed for the implied fading of bright rays over time were solar radiation, cosmic-ray bombardment, and micrometeorite mixing with the darker substrate (Shoemaker, 1962b, p. 345; Shoemaker and Hackman, 1962, p. 299). Chapter 5 explained that the main darkening agent proved to be the accumulation of Fe- and Ti-rich agglutinates generated in the regolith by small impacts at the expense of brighter crystalline material. Rays that cross mare regoliths rich in these agglutinates are less conspicuous than those superposed on mare and terra materials that are poor in Ti and Fe.

The interiors of Eratosthenian craters smaller than about 8 km in diameter commonly are more nearly V-shaped than are both older and younger craters of the same size (figs. 10.41, 12.3, 12.5–12.7). Imbrian craters are shallower and commonly more nearly U-shaped (figs. 10.38, 10.41). Many Copernican craters still display their original floor topography. These differences result from time-dependent filling of crater bottoms by debris from the walls. The best Orbiter resolutions show that Eratosthenian craters smaller than about 3 km in diameter are smoother than their Copernican counterparts. The

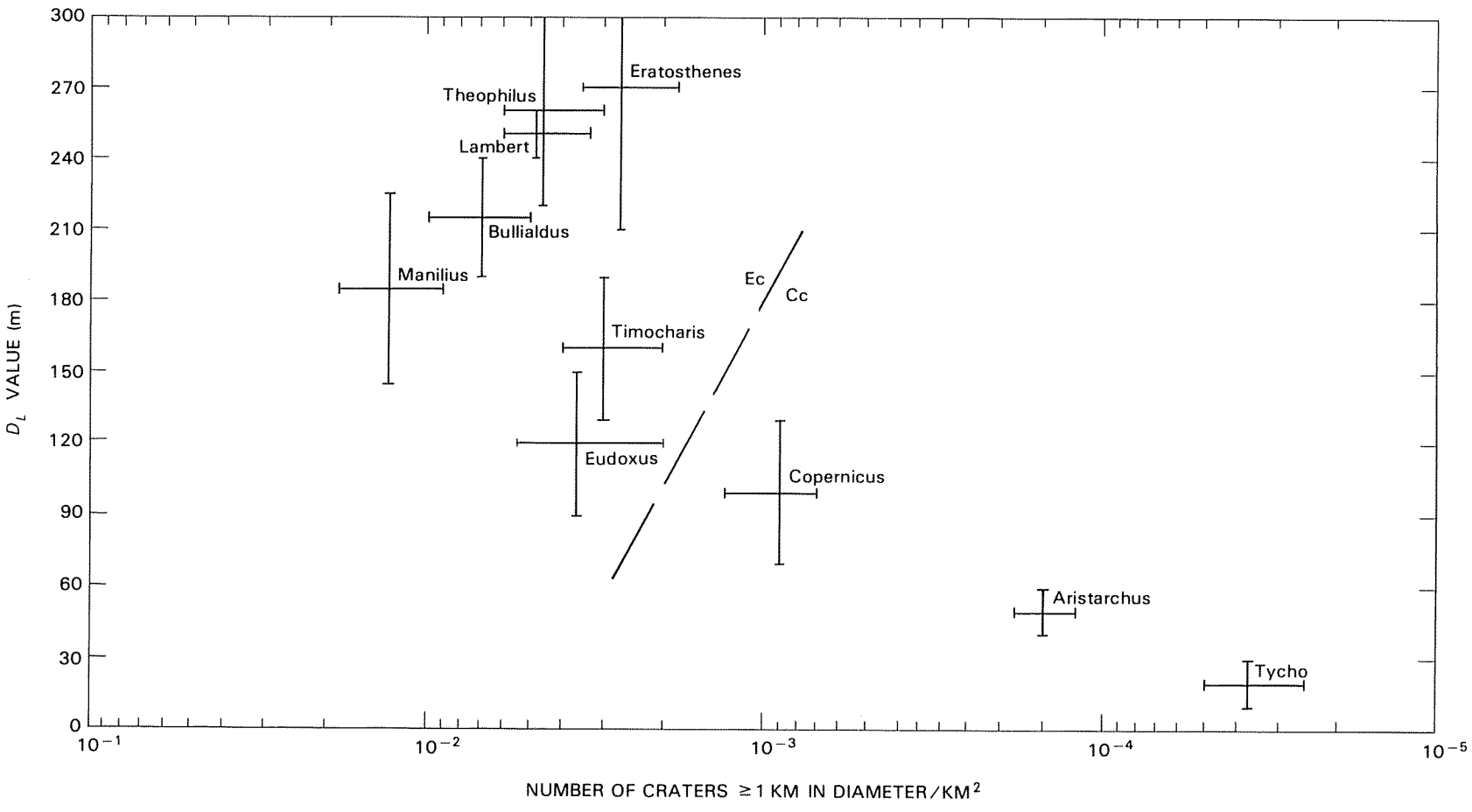

FIGURE 12.8.—Comparison of D_L values and frequencies of small (min 1 km diam) craters superposed on crater materials, based on figure 12.4 and table 12.3. Cc, Copernican craters; Ec, Eratosthenian craters.

oldest Eratosthenian craters disappear completely at sizes of about 300 to 400 m, and the youngest at about 75 m (fig. 7.14).

In summary, crater units of the Eratosthenian System are best recognizable where fine-scale features are visible: morphologies and frequencies of small superposed craters, fine-scale smoothing by invisible craters in the steady state, and superpositional relations with mare flows. The brightness of a ray is a function not only of its age but also of the material in which the ray-forming secondary craters were excavated. Better data might require revision of some of the age assignments given here (pl. 10), particularly on the farside and on the north, south, and east limbs of the nearside.

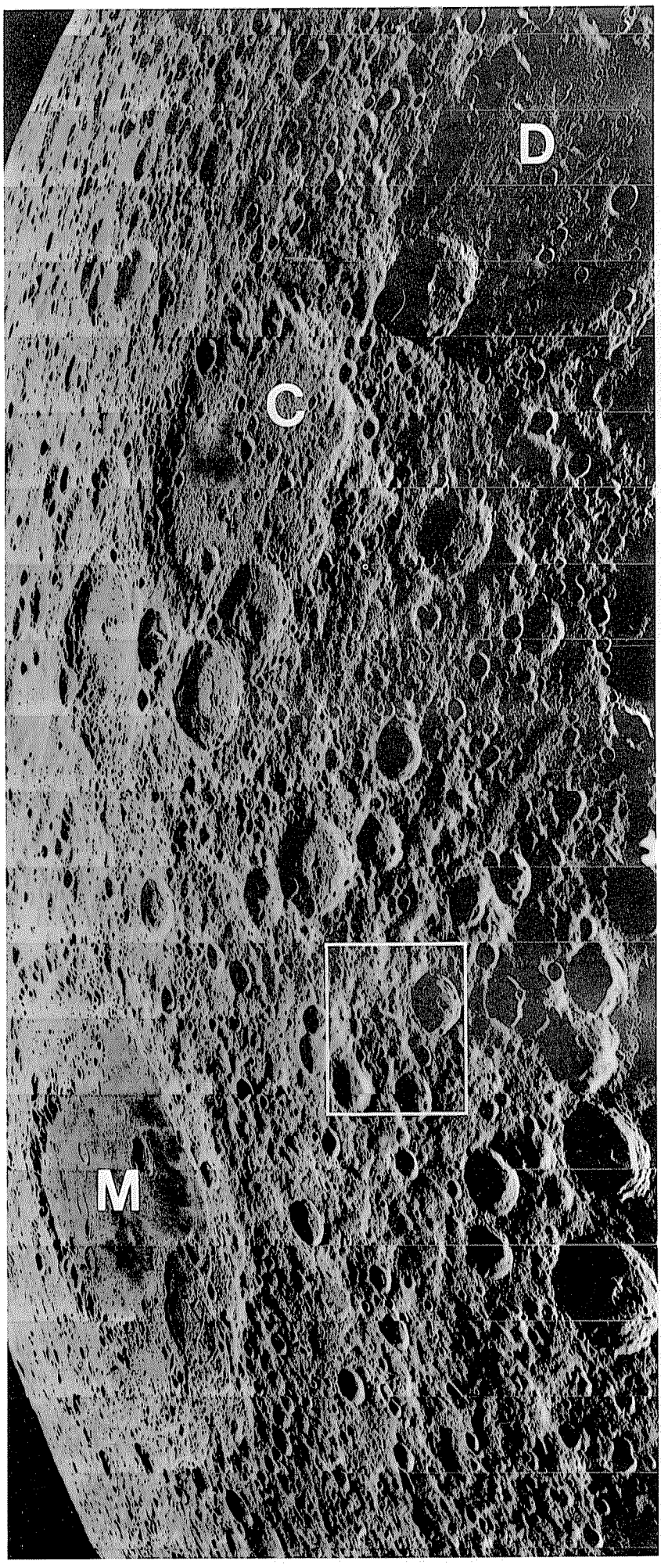

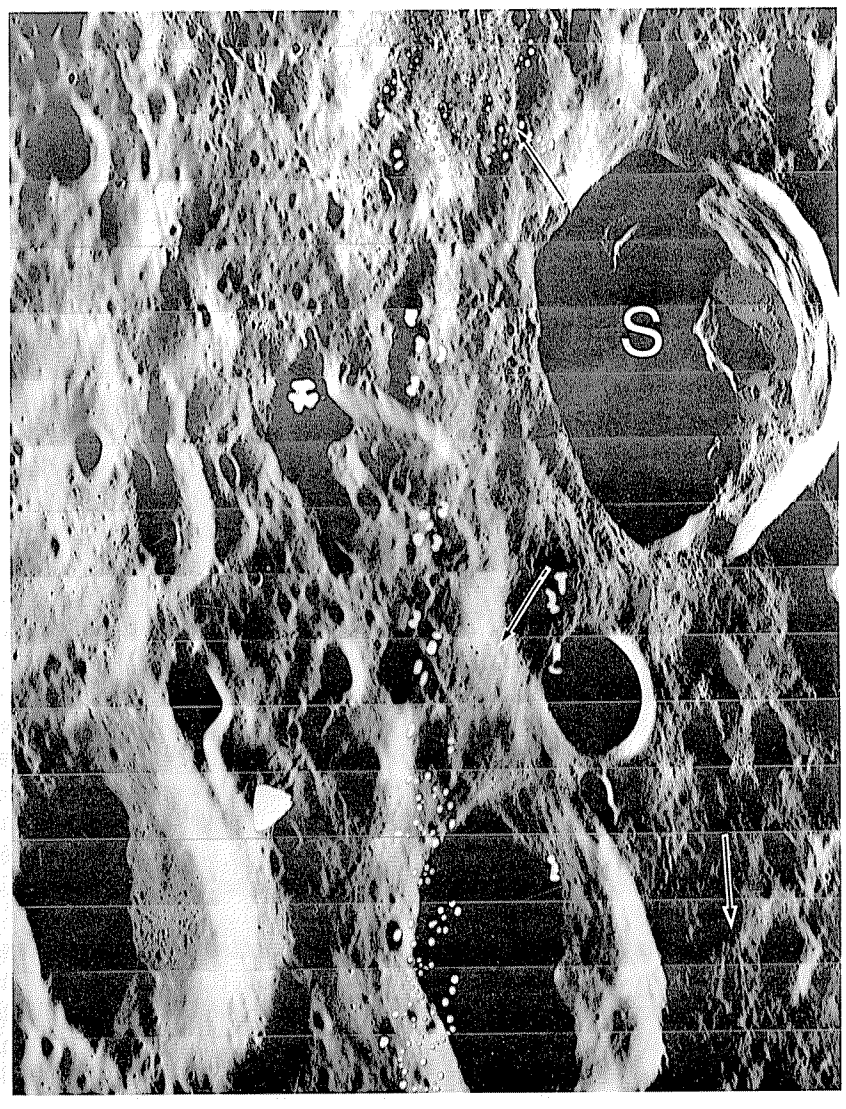

FIGURE 12.9.—Crater Stearns (S, 37 km) on lunar farside, identified as Eratosthenian by topographic sharpness.

A. Stearns inside box (*B*). Basin partly filled by mare is Moscoviense (M; 26° N., 147° E.). Large craters are Campbell (C; 225 km, probably pre-Nectarian) and D'Alembert (D; 225 km, probably Nectarian). Orbiter 5 frame M–85.

B. Freshness of Stearns' (S) interior is evident, despite oblique viewing angle and obscuration by shadow. Smoothed radial ejecta and secondary craters are also preserved (arrows), despite rugged terra substrate; periphery of Stearns is pitted by small craters. No exterior textures would be visible around an Imbrian crater of same size and setting; fewer pits and sharper texture would characterize Copernican craters of same size and setting. Orbiter 5 frame H–85.

Frequency

Application of these qualitative criteria apparently has resulted in fairly consistent age assignments, judging by the even densities on the paleogeologic maps (pls. 10, 11) of Eratosthenian and Copernican craters larger than 30 km in diameter. A total of 88 Eratosthenian craters of this size are recognized.

Wilhelms and McCauley (1971) mapped 256 Eratosthenian craters larger than 10 km in diameter within an area of 12.07×10^6 km^2. In the same area, they mapped 145 Copernican craters of these sizes. Their criteria differed somewhat from those used here because brightness depends partly on substrate composition and because some sharp craters thought to be primary are actually secondary-impact craters (Wilhelms, 1976). Nevertheless, the criteria were applied consistently, and no more complete compilation of craters of this size exists. Smaller craters were mapped at 1:1,000,000 and larger scales, but total numbers or frequencies have not been determined; such an exercise would suffer from greatly differing data quality, the effects of differing substrates, and subjective differences among mappers.

Wilhelms and others (1978) determined the frequencies of Eratosthenian and Copernican craters, combined, larger than 4.5 km in diameter (fig. 7.16); craters of these two systems were not distinguished because of the uneven quality of data in the area studied. The slope of the cumulative-frequency curve that best fits postmare craters 10 to 80 km in diameter is −1.8 (Baldwin, 1964; Shoemaker, 1965; Neukum and others, 1975a; Basaltic Volcanism Study Project, 1981, p. 1051–1052). Slopes of the curves for smaller craters depend on diameter range, as shown in figures 7.10*G* and 7.16.

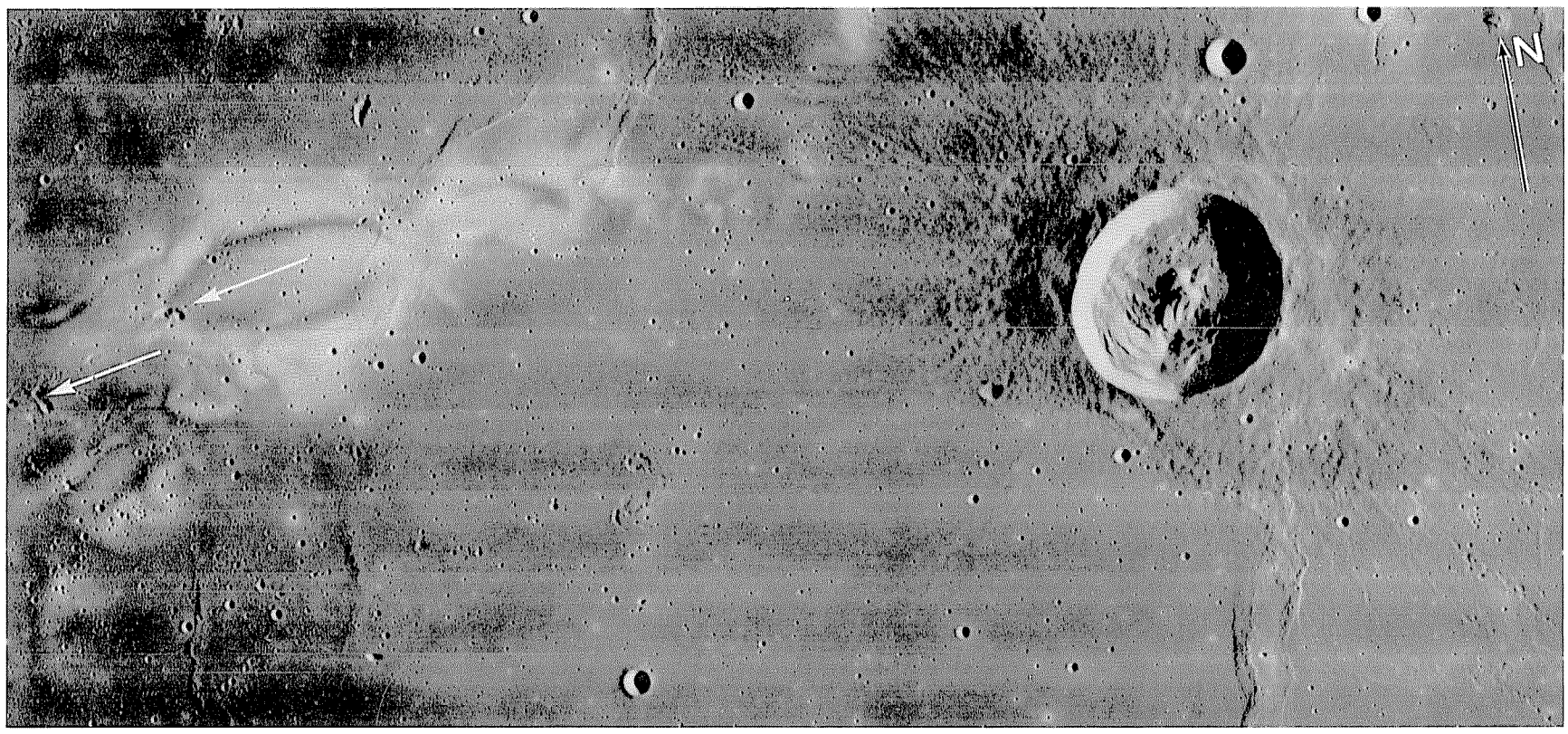

FIGURE 12.10.—Reiner gamma (tadpole-shaped bright patch). Arrows indicate secondary craters of crater Cavalerius, centered 220 km away in direction of arrows. Conspicuous crater is Reiner (30 km), whose superposition on mare material indicates Eratosthenian or Late Imbrian age; pinch in ejecta pattern northeast and southwest of crater is probably due to oblique impact (see chap. 3), but possibly is due to embayment by younger (Eratosthenian) mare. North arrow is adjacent to part of Marius Hills (see chap. 5). Orbiter 4 frame H–157.

MARE MATERIALS—GENERAL STRATIGRAPHY AND DISTRIBUTION

Eratosthenian mare units occupy two main settings—central Mare Imbrium and a crescentic zone extending from Mare Frigoris to southern Oceanus Procellarum (pl. 10; figs. 12.1, 12.3, 12.5–12.7, 12.11). The Imbrium and Procellarum tracts join in a zone south of Montes Harbinger. Smaller patches of Eratosthenian basalt are scattered in the rest of Oceanus Procellarum and in other maria.

The massive, dark, spectrally blue flows in Mare Imbrium described in chapter 5 extend northeastward from the connection with Oceanus Procellarum—near the edge of Mare Imbrium—to a point north of the Imbrium center (fig. 5.1; Schaber, 1969; Schaber and others, 1975). Their stratigraphic relations are among the Moon's clearest because they flood small and large Eratosthenian craters and cover Imbrian mare units (figs. 12.1, 12.5; Wilhelms, 1980). Before the Apollo missions, an Eratosthenian age was also established for mare units in a large area of equatorial Oceanus Procellarum by superpositional relations with small craters (fig. 12.6) and by evidence that the regolith there is thin. Thin regolith was indicated by the blocky surface revealed by Surveyor 1 at one point within this area (Shoemaker and Morris, 1970; Offield, 1972) 1970), and by an abundance of small blocky craters (Trask, 1969, 1971) and certain nested-crater configurations (Oberbeck and Quaide, 1968; Quaide and Oberbeck, 1968, 1969) that are visible on high-resolution Lunar Orbiter photographs over extensive additional parts of the area. Several sites within the area were considered for Apollo landings because of the mare's youth (Carr and Titley, 1969; Titley and Trask, 1969; Cummings, 1971; West and Cannon, 1971; Offield, 1972). Many flows in northern Oceanus Procellarum are also young; some west of the Aristarchus Plateau are only about twice as old as the crater Copernicus (Young, 1977).

The most extensive Eratosthenian mare units of Mare Imbrium and Oceanus Procellarum are spectrally blue and, thus, probably rich in Fe and Ti (see chap. 5); they also are more radioactive than most other mare units (Soderblom and others, 1977). The most common spectral type is hDSA, although type HDSA is present in several spots in Oceanus Procellarum, including the Flamsteed-Flamsteed P region (pl. 4; fig. 12.6; table 5.1; Pieters, 1978; Pieters and others, 1980). The spectral class (hDSA) and gamma-ray-spectrometer readings of the massive Imbrium flows indicate Ti contents in the range of about 2.0 to 4.5 weight percent TiO_2 (Pieters, 1978; Davis, 1980). Small patches of Eratosthenian flows, most spectrally blue but some red, are scattered throughout southern Oceanus Procellarum and Maria Insularum and Nubium (pl. 10; Whitford-Stark and Head, 1980). Similar patches, including several with red spectra (Wilhelms, 1980), are scattered between long 25 W. and the central highlands "backbone" (fig. 1.8; see chap. 11).

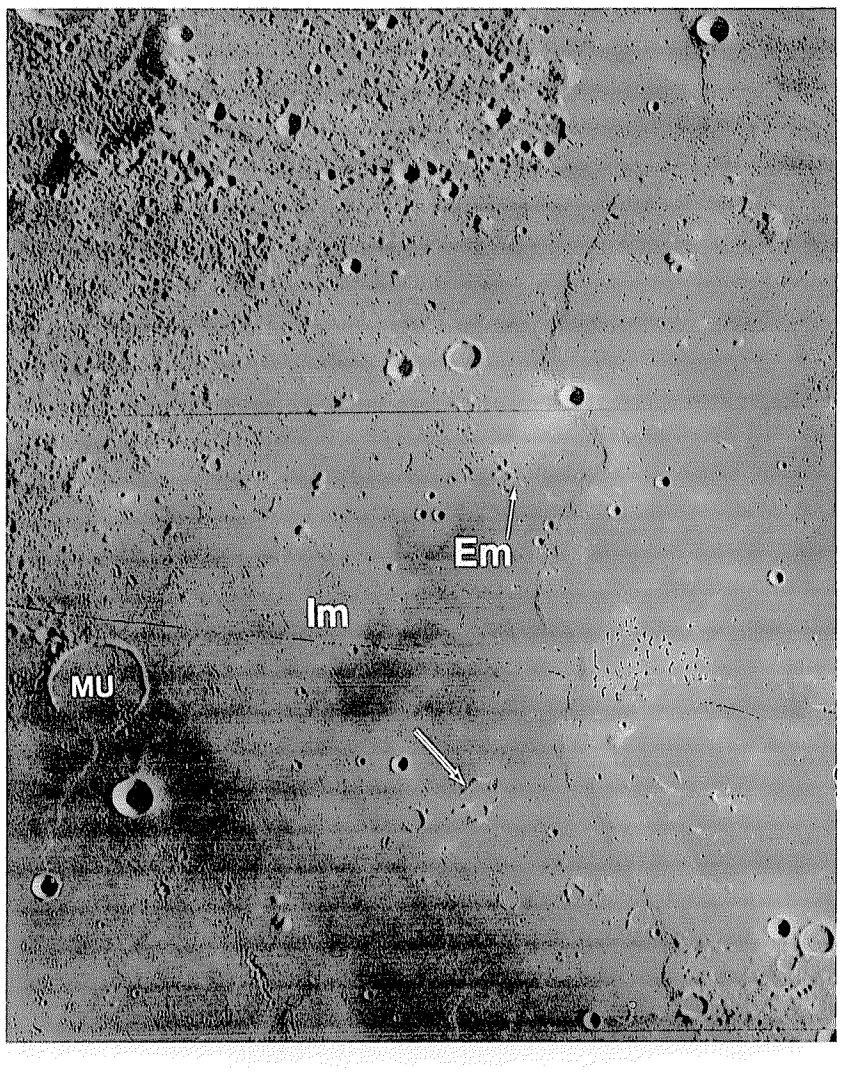

FIGURE 12.11.—Sinus Roris, showing flooding of Imbrian mare materials (Im) by dark, thin Eratosthenian mare materials (Em). Secondary craters of Eratosthenian crater Pythagoras (out of scene to upper left) overlie Imbrian units but are truncated by Eratosthenian unit (white arrow). Both mare units flood secondary craters of Iridum crater (black-and-white arrow). Large crater flooded by Imbrian units is Markov U (MU; 29 km, 52° N., 60° W.). Orbiter 4 frame H–170.

The most abundant spectrally red Eratosthenian flows are on opposite sides of the ring of the Imbrium basin that is overlain by the Iridum crater and Plato. The flows on the Mare Imbrium side are beyond the margins of the spectrally blue Imbrium flows (compare pls. 4, 10).

I suggest that the concentration of Eratosthenian as well as Imbrian eruptions in the Imbrium-Procellarum region is due to the thin lithosphere beneath the Procellarum basin (fig. 11.14). Conditions elsewhere also favored local late eruptions, however, judging by some patches of young basalt in Mare Smythii and other outlying maria (Boyce and Johnson, 1978). The factors controlling the distribution of spectral types are unclear. The main reason that high-Ti basalt dominates the Eratosthenian System may be its high radioactivity; the requisite heat for longlasting melting was greatest in this compositional type (Taylor, 1975, 1982).

Many of the Eratosthenian flows occupy, or flowed from, the margins of several maria in addition to Imbrium (pl. 10; Boyce and Johnson, 1978). Small patches are perched high on the peripheries of Imbrium, Serenitatis, Crisium, and, probably, other basins (figs. 5.10*D*, 5.16, 5.25). Solomon and Head (1980) suggested that the changing lunar stress pattern resulting from global cooling and consequent lithospheric thickening favored closing of conduits everywhere except at mare margins. However, the thick existing sections of Imbrian basalt in the basin centers may have deflected the rising Eratosthenian magmas to the mare margins.

MARE INSULARUM

Setting of the Apollo 12 landing site

Apollo 12 landed in a topographically complex region, rich in islands of terra material, which at that time (November 1969) was considered part of Oceanus Procellarum but is now known as Mare Insularum (lat 3.2° S., long 23.4° W.; pl. 1; fig. 12.12; U.S. National Aeronautics and Space Administration, 1970; Marvin and others, 1971). As mentioned above, the existence of the blue Eratosthenian mare material in the west-central equatorial belt of the nearside was known when the site was selected. These maria were called "western," as opposed to the "eastern" maria east of long 25° W., which are mostly Imbrian. After the succesful Apollo 11 mission to an "eastern" site, geologists wanted to explore a "western" mare. However, the Apollo 12 landing site ended up being selected entirely for operational reasons. The desire was to demonstrate the ability of the Apollo system to land a LM at a predesignated point, and the Surveyor 3 spacecraft, which had landed 2½ years earlier, provided an appropriate target. Surveyor 1 farther to the west offered a similar target, and its site was called Apollo landing site 6; but complex requirements of launch opportunity and other factors favored the Surveyor 3 site. As predictable from its position near the 25° W. dividing longitude, the geologic context of the site is less well known than that of the Eratosthenian Surveyor 1 mare (Offield, 1972).

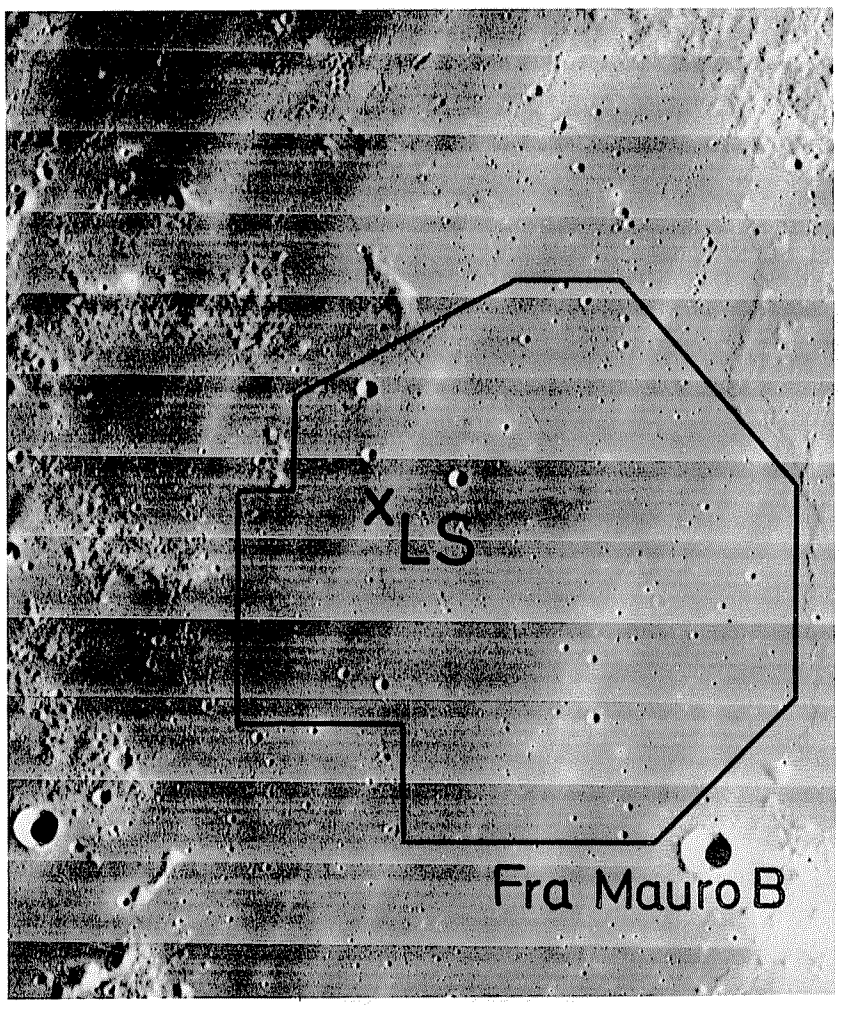

FIGURE 12.12.—Area around Apollo 12 landing site (LS) whose size-frequency distribution was determined by Neukum and others (1975b). Two units (at least) were included in counts (fig. 11.2*B*); less densely cratered unit around landing site gives lower frequency plotted in figure 11.2*B*. Fra Mauro B is 7 km across. Courtesy of Gerhard Neukum. Orbiter 4 frame H–125.

The vicinity of the landing site and almost all the sampled terrain are occupied by the interiors or ejecta of several large craters (figs. 12.13–12.15). Most of this area is theoretically within the ejecta blanket of the largest of these, Middle Crescent Crater, 400 m across and originally about 80 m deep (Sutton and Schaber, 1971). Surveyor Crater (the 200-m crater in which Surveyor 3 landed) and Head Crater (110 m, the head of a crater configuration that resembles a snowman) also have strongly influenced the site. Samples were also taken from several spots on the ejecta of Bench Crater and near Halo Crater (fig. 12.14).

The overlapping ejecta blankets contribute to considerable uncertainty about the source strata of the basaltic samples and the significance of remotely sensed spectra. A spectrum centered over the landing site is of type mIG-, that is, intermediate in Ti, intermediate in albedo, and average or lacking in the two long-wavelength absorption bands (Pieters and McCord, 1976; Pieters, 1978). The TiO_2 content of 2 to 3 percent suggested by this spectrum approximately matches that of the average regolith sample and falls between those of the two main types of sampled basalt. This averaging is expectable wherever surface deposits are composed of the ejecta blankets of craters that penetrate more than one unit. The crater frequencies and D_L values that characterize the sampled material are also unclear because the few named craters dominate the local crater population. Soderblom and Lebofsky (1972) suggested that two units are present in the general vicinity—an older unit at the site proper and a younger one about 1 km both west and east of the site. The unit at the site proper has a D_L value of 210 to 215 m (table 11.1; Soderblom and Lebofsky, 1972; Boyce, 1976). The D_L value of the other unit is smaller by an undetermined amount (Soderblom and Lebofsky, 1972). These values fall in the Eratosthenian System as defined here. The midpoint of size-frequency counts in the unit at the site is 2.4×10^{-3} craters larger than 1 km in diameter per square kilometer (table 11.1, figs. 11.2, 12.12). The relative and absolute ages are the youngest from any sampled mare site, including the Apollo 15 units, which lie near the top of the Imbrian System. Therefore, I consider the Apollo 12 mare materials to be Eratosthenian.

Apollo 12 samples

A total of 36 rock-size basalt samples were returned by Apollo 12 (Warner, 1971; James and Wright, 1972). Four compositional types of basalt have been recognized, starting with the early studies. They are now thought to compose two major and one minor unit at the site (Rhodes and others, 1977).

Olivine and pigeonite basalt.—Two of the compositional groups—olivine basalt characterized by modal olivine, and pigeonite basalt characterized by especially abundant modal pigeonite—are probably parts of the same flow, which fractionated at the surface or in a shallow magma chamber (James and Wright, 1972; Rhodes and others, 1977). The pigeonite basalt has the finer textures, which indicate more rapid cooling, and so is presumably the upper fraction of the flow. The distribution of samples near the landing site is consistent with this stratigraphic relation (Rhodes and others, 1977). The olivine basalt apparently was excavated only by the largest crater, Middle Crescent (original depth, approx 80 m; fig. 12.15), whereas the smaller crater, Surveyor (original depth, approx 40 m), excavated the pigeonite basalt but not the olivine basalt.

The radiometric ages of samples of these two compositional groups have about the same broad range (table 12.4). Rb-Sr ages from a given laboratory favor an age 0.1 aeon older for the olivine than for the pigeonite basalt—3.25 versus 3.15 aeons (Papanastassiou and Wasserburg, 1970, 1971a), or 3.22 versus 3.12 aeons (Nyquist and

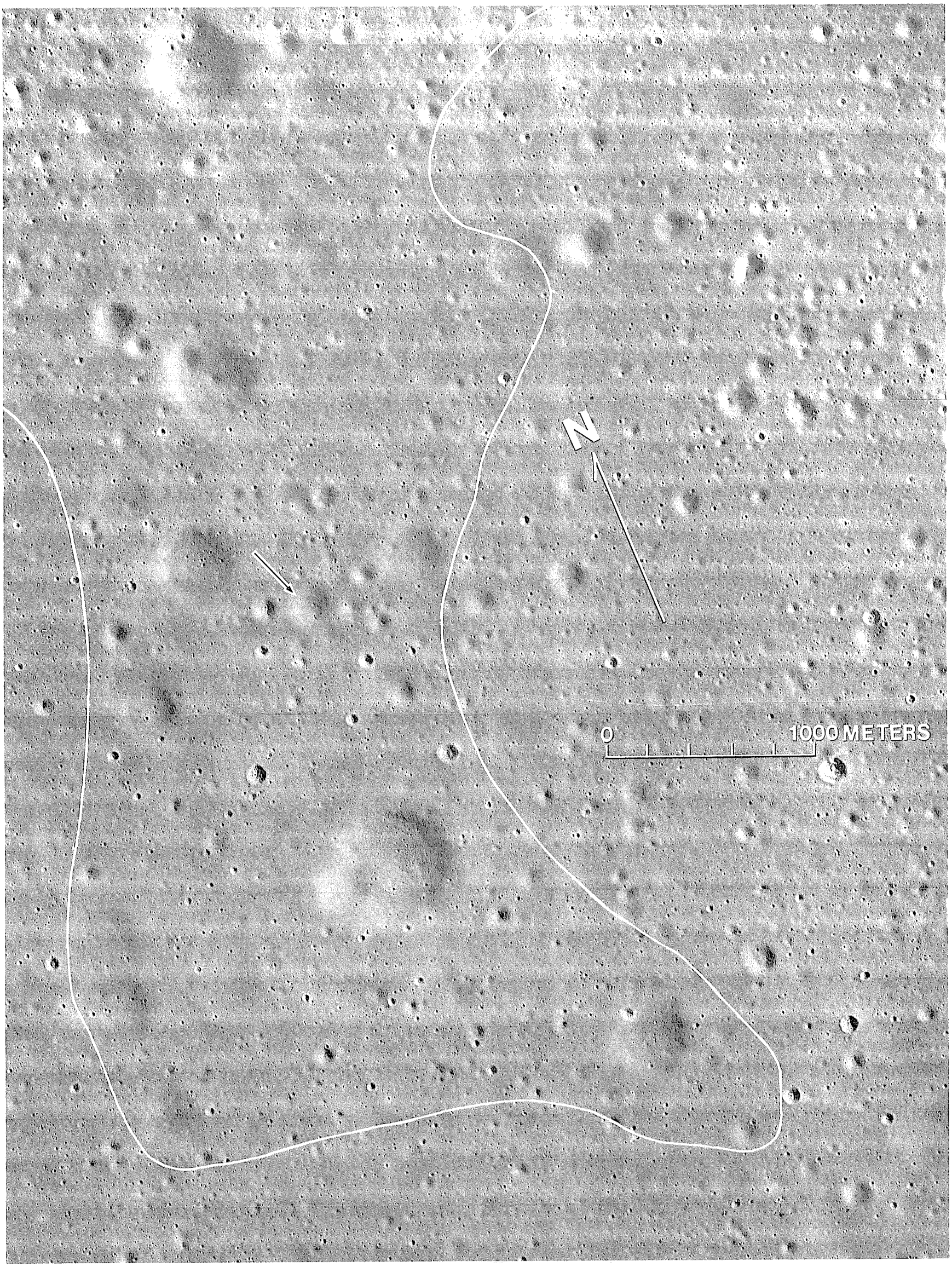

FIGURE 12.13.—Apollo 12 landing site and vicinity. Arrow marks location of Lunar Module in Surveyor Crater. Mare unit around landing site contains more large, subdued, old craters than unit outside line and thus is the older unit. Orbiter 3 frame H–154.

others, 1977, 1979a). The fewer Ar-Ar ages cluster more tightly, however, and those determined by Turner (1971, 1977) in each group are the same—3.21 aeons. In view of the overlapping analytical errors and the inconsistent discrepancies between the two methods (for example, sample 12065 is older by Ar-Ar, and sample 12002 older by Rb-Sr), the absolute ages may be considered consistent with the chemical, textural, and petrologic evidence for a common origin of the two compositional groups (James and Wright, 1972; Rhodes and others, 1977). Rhodes and others (1977) estimated a flow thickness of 30 to 50 m. The average age for the combined compositional groups, from determinations whose stated error ranges are less than 0.1 aeon, is 3.16 aeons, which is adopted here as the age of the flow.

Ilmenite basalt.—The ilmenite basalt contains 2.7 to 5.5 weight percent TiO_2, more than the other Apollo 12 groups, though less than many mare-basalt samples from other sites. Accordingly, it has been called either "low-Ti basalt" or "intermediate-Ti basalt" (table 5.2). Ilmenite basalt has been considered a minor component near the landing site, possibly introduced in crater ejecta from a nearby Ti-rich spectral unit approximately corresponding to the younger unit recognized by Soderblom and Lebofsky (1972). In this interpretation (Pieters and McCord, 1976), the olivine-pigeonite flow would be the local bedrock at the landing site. However, the restudy by Rhodes and others (1977) of the surficial distribution of recovered samples showed that ilmenite basalt is, in fact, quite common among the rock-size samples and is probably local to the site. The ilmenite basalt is apparently the only inplace basalt excavated by craters smaller than Surveyor, such as Head, whose original depth was about 20 m, whereas only the larger Surveyor and Middle Crescent Craters excavated inplace olivine and pigeonite basalt (fig. 12.15). Although the smaller craters also reejected some fragments of the olivine-pigeonite flow, these fragments resided in the ejecta of the larger craters. Therefore, the ilmenite basalt flow overlies the olivine-pigeonite flow. On the basis of the likely original penetration depths of the craters (fig. 3.3), Rhodes and others (1977) estimated that the ilmenite basalt flow is about 40 m thick. Compositional data indicate derivation of this flow from a different magma from the parent magma of the olivine and pigeonite groups, which originated in a different mantle source (James and Wright, 1972; Rhodes and others, 1977). However, the ages for the ilmenite basalt listed in table 12.4, which average 3.15 aeons from the best determinations, indicate no large gap between times of eruption of the two magmas.

Feldspathic basalt.—Only one or, possibly, two rock-size samples of Al-rich, feldspathic basalt were recovered (12031?, 12038). The Rb-Sr ages overlap those of the other groups. The average of the best Rb-Sr age determinations (stated error ranges, less than 0.1 aeon) and the one young Ar-Ar age (3.08 aeons) is, again, 3.16 aeons. The petrologic relation of the feldspathic basalt to the other compositional groups is uncertain (Rhodes and others, 1977). The paucity of samples suggests a provenance in a distant unit or in a deeply buried unit at the landing site proper. The latter view (Nyquist and others, 1981b) is supported by collection of sample 12038 from the largest crater, Middle Crescent (by way of the superposed Bench Crater). Nyquist and others (1981b) favored derivation of this and other aluminous mare basalt from sources containing plagioclase in addition to the olivine and pyroxene generally thought to compose mare-source zones.

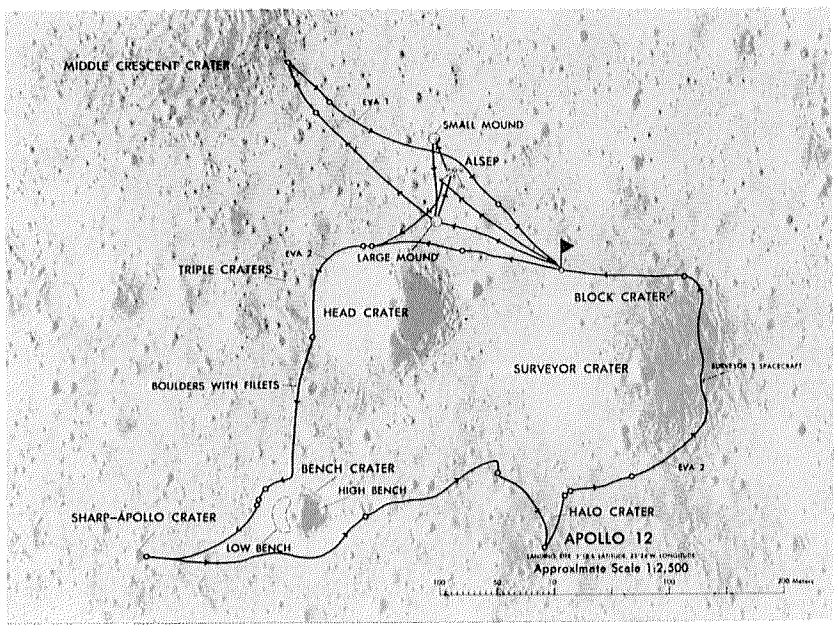

FIGURE 12.14.—Astronaut traverses at Apollo 12 landing site. Small circles, sampling localities; pennant, landing site; ALSEP, geophysical instruments. Airbrush map by U.S. Geological Survey.

TABLE 12.4.—*Radiometric ages of large Eratosthenian basalt samples*

[All ages in aeons, recalculated using the radioactive-decay constants recommended by the International Union of Geological Sciences (IUGS) (Steiger and Jäger, 1977).
References: AD74, Alexander and Davis (1974; incorporates revisions of earlier determinations by the same laboratory [University of California, Berkeley], which are not given here); BB1, Basaltic Volcanism Study Project (1981, p. 950–952, table 7.3.1); C71, Cliff and others (1971); Co71, Compston and others (1971), as modified by de Laeter and others (1973); H75, Horn and others (1975); Murthy and others (1971); N77, Nyquist (1977); N79a, Nyquist and others (1979a); N81b, Nyquist and others (1981b); PW70, Papanastassiou and Wasserburg (1970); PW71a, Papanastassiou and Wasserburg (1971a); PW71b, Papanastassiou and Wasserburg (1971b); S73, Stettler and others (1973); T71, Turner (1971); T77, Turner (1977)]

Group	Sample	Station	Rb-Sr age (reference)	Ar-Ar age (reference)	Sm-Nd age (reference)
Apollo 12 feldspathic basalt.	[1]12031	N. rim of Head--------	3.13±0.03 (N81b), 3.16±0.07 (N79a).	---	---
	12038	SW. of Bench----------	3.23±0.04 (BB1), 3.28±0.09 (N81b).	[2]3.08±0.05 (T77)	3.28±0.23 (N81b)
Apollo 12 ilmenite basalt.	12022	NE. of Head----------		3.08±0.04 (AD74)	---
	12051	S. rim of Surveyor----	3.09±0.04 (N77), 3.19±0.10 (PW70, PW71a).	3.13±0.06 (S73), 3.21±0.05 (AD74), 3.23±0.05 (T71).	---
	12056	SE. rim of Surveyor----------			3.20±0.14 (N81b)
	12063	Block (NE. rim of Surveyor).	3.23±0.13 (PW71a), 3.27±0.10 (M71).	3.15±0.05 (T77)	---
Apollo 12 pigeonite basalt.	12017	NE. of Head----------		3.16±0.07 (H75)	---
	12021	NE. of Head----------	3.23±0.10 (C71), 3.26±0.06 (PW71a).	---	---
	12039	SW. of Bench----------	3.12±0.06 (N77), 3.13±0.03 (N81b).	---	3.20±0.15 (N81b)
	12052	W. rim of Head--------	3.15±0.19 (Co71)	---	---
	12053	N. rim of Bench----------		3.14±0.06 (H75)	---
	12055	N. rim of Head--------	3.12±0.06 (N77), 3.13±0.03 (N81b).	---	---
	12064	SE. rim of Surveyor---	3.11±0.09 (PW71a)	3.15±0.04 (H75)	---
	12065	SE. rim of Surveyor---	3.09±0.09 (PW71a)	3.13±0.04 (AD74), 3.21±0.05 (T71)	---
Apollo 12 olivine basalt.	12002	SE. rim of Middle Crescent.	3.29±0.10 (PW70, PW71a)	3.18±0.04 (AD74), 3.21±0.05 (T71)	---
	12004	NE. of Head----------	3.22±0.07 (PW71b)	---	---
	12014	NE. of Head----------	3.22±0.11 (N79a, N81b)	---	---
	12020	SE. rim of Middle Crescent.	---	3.09±0.04 (AD74)	---
	12040	SW. of Bench----------	3.08±0.10 (Co71), 3.23±0.04 (PW71a).	---	---

[1]Nyquist and others (1981b) considered this sample to be pigeonite basalt.
[2]Nyquist and others (1981b) believed that this age is too young because of disturbance of the argon system.

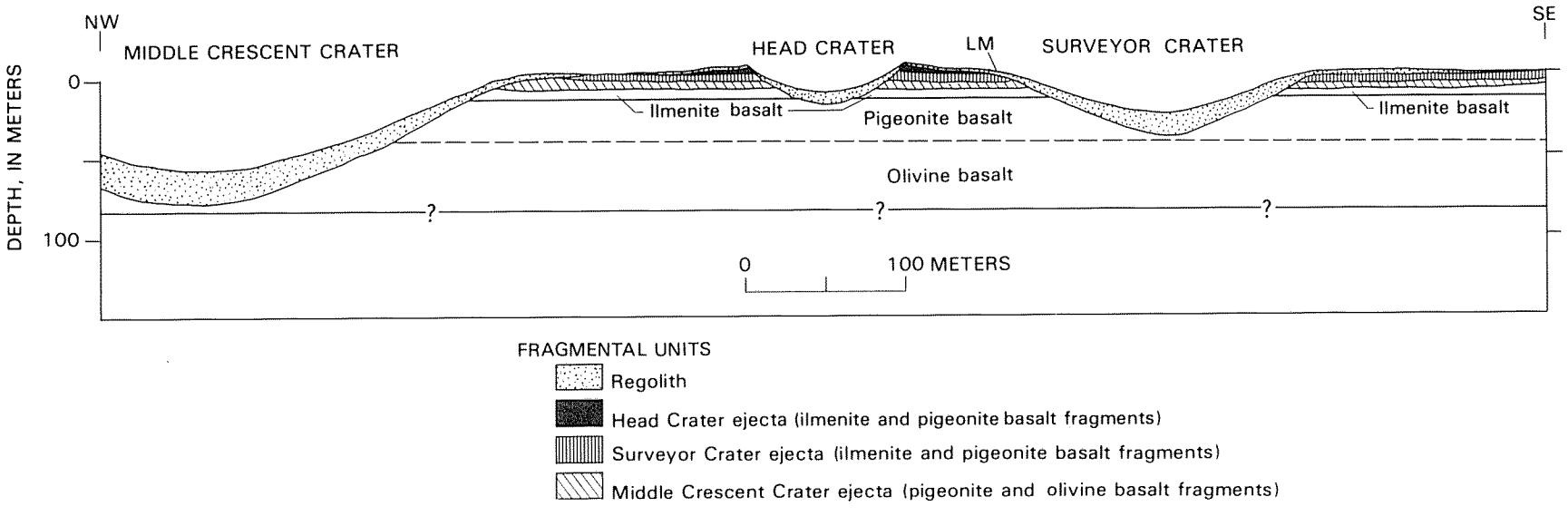

FIGURE 12.15.—Geologic cross section northwest-southeastward across area sampled by Apollo 12 (compare fig. 12.13). Interpretations after Sutton and Schaber (1971) and Rhodes and others (1977). Substrate of Fe-Mg-rich basalt may be another mare unit or Fra Mauro Formation.

Summary and conclusions

The best determined ages on Apollo 12 samples cluster between 3.08 and 3.26 aeons and average 3.16 aeons. The stratigraphic sequence, from lowest to highest, is olivine basalt, pigeonite basalt, and ilmenite basalt. The bottom two compositional groups are parts of the same flow, and the ilmenite basalt is from a different flow. Absolute ages of these compositional groups or of the rare feldspathic basalt, whose provenance is uncertain, are indistinguishable.

Each mare-sampling site has increased our knowledge of the petrogenetic processes and source materials of lunar mare basalt after intensive and diligent study lasting more than a decade. After Apollo 11, there was talk of a single episode of mare extrusion; after Apollo 12, the number of episodes rose to two; and after each subsequent mission, the history of lunar volcanism appeared increasingly complex. We should, therefore, be chastened by the fact that at least two-thirds of the major mare spectral types remain unsampled (Pieters, 1978).

In particular, Pieters (1978) cautioned against drawing conclusions about the rather poorly defined spectral class (mIG-), to which the Apollo 12 basalt samples apparently belong. This class of material is widespread on the Moon (pl. 4) and contains many age and spectral subunits. Nevertheless, its general distribution may be of interest in attempts to discern first-order features of the lunar crust. It lies in areas of known thick crust outside the Procellarum basin (Crisium, Fecunditatis), as well as inside Procellarum in zones nearest the central terra "backbone." Eratosthenian basalt is also less abundant there than elsewhere in Procellarum. Therefore, the lithosphere may have been thicker, and the crust or upper mantle different in composition, here than elsewhere in southern, western, and northern Procellarum, where Ti-rich basalt flows are abundant. The unusual north-south trend of the Eratosthenian patches and of such terra features as the "Fra Mauro peninsula" and the "central backbone" itself (fig. 1.8) may be additional evidence for a major structural trend along the central meridian of the nearside.

CHRONOLOGY

The Apollo 12 basalt flows, which lie near the base of the Eratosthenian System, average about 3.16 aeons in age. No younger or older Eratosthenian materials were sampled, and so absolute ages of other Eratosthenian units must be extrapolated from the dated samples by means of superposed-crater frequencies and D_L values. The Eratosthenian Period began some time between 3.16 aeons ago and the 3.26-aeon formational time of the youngest Apollo 15 basalt samples. An approximate intermediate date of 3.2 aeons ago is adopted here.

The end of the Eratosthenian Period is harder to estimate. As discussed in detail in the next chapter, a date of 1.1 aeons is adopted on the assumption that the cratering rate has been constant since 3.2 aeons ago. Thus, in this hypothesis, the Eratosthenian Period lasted 2.1 aeons—the longest of the six lunar time divisions adopted in this volume and nearly half the age of the Moon.